Reykjavik University

Implementation of a new energy storage system for a high altitude long endurance aircraft

Stefanie Dagner

Master of Science in Sustainable Energy Engineering – ISE

Thesis of 60 ECTS credits

January 2015

Reykjavik University

Implementation of a new energy storage system for a high altitude long endurance aircraft

Stefanie Dagner

Thesis of 60 ECTS credits submitted to the School of Science and Engineering at Reykjavik Universoty on partial fulfillment of the requirements for the degree of Master of Science in Sustainable Energy

January 2015

Supervisor: **Ágúst Valfells**
Professor, Reykjavík University, School of Science and Engineering

Examiner: **Ármann Gylfason**
Professor, Reykjavík University, School of Science and Engineering

Implementation of a new energy storage system for a high altitude long endurance aircraft

Stefanie Dagner

Thesis of 60 ECTS credits submitted to the School of Science and Engineering at Reykjavik Universoty on partial fulfillment of the requirements for the degree of Master of Science in Sustainable Energy

January 2015

Student: _____

Signature Student

Supervisor: _____

Signature Prof. Ágúst Valfells

Examiner: _____

Signature Prof. Ármann Gylfason

Abstract

In future solar powered high altitude long endurance (HALE) aircrafts shall be used to replace satellites. They could fulfill the same tasks satellites have to fulfill nowadays, just that HALE aircrafts are lighter and cheaper.
In this project a high altitude long endurance aircraft and its energy source are examined. By using solar panels, it collects the energy over the day - for immediate use and to store the surplus in batteries for the night flight. The battery system with just a short lifetime contributes a lot to the endurance of the flight, so there is space for improvement.
After sizing a proper original model, consisting of Lithium-ion batteries as energy storage system, there are introduced several new energy storage models to replace the original model. The total aircraft weight, power demand of the aircraft, designs of the solar cell system and the energy storage system and lifetimes of the different models are determined. After that, a recommendation for a replacement for the original energy storage model is given.
The recommendation is to use a combination of proton exchange membrane fuel cells and super capacitors as energy storage system. The energy storage system consists of 60 % of proton exchange membrane fuel cells and 40 % of super capacitors. Here the best results for lifetime of the energy storage system as well as the storage system's weight and the total weight of the aircraft are achieved.

Keywords: *High Altitude Long Endurance Aircraft, Energy Storage System, Solar Power, Drag, Lift, Super capacitor*

Contents

List of Figures

List of Tables

Chapter 1

Introduction

1.1 Motivation

The development of solar powered **H**igh **A**ltitude **L**ong **E**ndurance (HALE) aircraft has a great impact on both military and civil aviation industries since its features in high altitude and energy source can be considered inexhaustible. Owing to the development constraints of rechargeable batteries, Lithium-ion batteries in this paper, the solar powered HALE aircraft must take an amount of rechargeable batteries to fulfill the energy requirement during the night, which greatly limits the operation altitude of the aircraft.

The civil applications have a much larger scope than the military use. The HALE aircraft could be used for several civilian applications like surveillance, communication, scientific research and remote sensing. Hence, a HALE aircraft could replace satellites in future. Since satellites are very heavy, big and expensive, the HALE aircraft has a clear benefit here. Normally, it is designed to be lightweight with just the minimum necessary equipment for the ongoing mission on board. The HALE aircraft flies in the stratosphere and provides a covered interest area of 100 km in diameter (e.g. relay services for wireless communication or mapping of a certain area of interest). HALE aircrafts are currently developed actively in a number of programs all around the world.

In this paper the focus was set on the battery system of the HALE aircraft. Possible substitutes were presented and evaluated due to their weight, lifetime and power demand from the solar cell system. Also the chances and obstacles of the possible substitutes for the original battery system are shown and discussed.

1.2 Objectives

The overall aim of this thesis is to create a HALE aircraft model and apply a different battery system. The paper can be split into two parts. The first part is to define an actual model of a high altitude long endurance aircraft and the second part is to replace the actual energy storage system by a different energy storage system to improve the actual one.
Specifically, the aims of this research for part one are to

(1) determine the forces acting on the aircraft,

(2) determine the engine size,

(3) determine the solar cell system,

(4) determine the battery system,

(5) determine the size, weight and stability of the aircraft and

(6) determine the mass of the whole structure.

After that, the objectives of this research for part two are to

(7) implement different energy storage systems existing of just one type of battery or combinations of these battery types,

(8) find out the new power needed from the solar cells, their amount and weight,

(9) determine the total weight of the aircraft with these new data,

(10) give an overview over the lifetimes of the different energy storage systems and

(11) give a comprehensible overview about these new developments and their benefits and obstacles.

Last but not least a proposal for the best energy storage system is given.

1.3 Methodology

This project has two main parts: first, the general sizing and development of the original model and second, the implementation of a new energy storage system.
The main sources of information, which were used for this project, were published papers, conference proceedings and several textbooks to certain contexts. Online sources provided some information, e.g. the web of science, the NASA website and the Journal of Powers, which were used in the main text.
In sizing part of this project, assumptions had to be made while keeping the most likely scenarios in mind. Therefore, often comparable data from satellites are used. An airfoil was chosen, which has already been used for an aircraft doing aerial photography and has good gliding characteristics. To find valid data for solar cells and the different energy storage systems, reliable data from up-to-date textbooks were used. With all these data the weight and stability of the HALE aircraft was determined.
In the implementing part of the project different models for a new energy storage system were stated. Therefore, reliable data were collected from textbooks. For all the models the needed solar power is calculated and a new mass statement with the necessary amount of solar cells was set up. A valid recommendation was made at last.

1.4 Outline of the thesis

In *Chapter 2* the general information are described. Here the terminologies regarding the HALE aircraft and its systems and components are mentioned and explained.
Chapter 3 outlines the sizing of the aircraft. Therefore, a proper airfoil was chosen and an estimate for the wing and fuselage size and shape was made. Also all important terminologies were explained. The needed power for the propulsion system is then determined and with this in mind the solar cell system and energy storage system for the original model were determined. At last, the weight and stability of the created model was calculated.
Chapter 4 provides different models as energy storage system substitutes. For all these models the power which is needed to be supplied by the solar cell system is calculated. Then the necessary amount of solar cells and their weight is determined. The lifetimes of the different models are also determined.
Chapter 5 states and explains the results from chapter 4 and also the results are discussed and a recommendation for the best choice(s) for a new energy storage system is given.
Chapter 6 concludes the thesis with a general overview over the HALE aircraft and its future.

Chapter 2

General information

2.1 High altitude long endurance (HALE) aircraft

High altitude long endurance (HALE) aircrafts can function as a low-cost alternative to satellites to fulfill certain space missions, such as telecommunication relay, environmental sensing and military reconnaissance. HALE missions require a light vehicle flying at low speed in the stratosphere at altitudes up to 20 km, with a continuous loiter time of one day up to several days, if possible. This HALE aircraft is unmanned which means it has some kind of autopilot system, which is pre-programmed, and the user could be anywhere in the world. So this aerial vehicle does not carry a human operator. According to the latest state of the art, the high altitude refers to a range between 15 to 20 km and the long endurance means at least 24 hours of continuous flight. Since the HALE aircraft using solar power it will not need to be refueled every now to then and theoretically fly for a virtually unlimited period of time. But of course this is not feasible nowadays. For a renewable energy HALE aircraft, regenerative power technologies are necessary such as an advanced energy storage system and thin film solar cells among others are the keys to achieve long endurance. Since the sun as power source is not available the whole day you can say the electrical energy system of the aircraft consists of three modules: [26] [69]

- Solar cells source module
  Here the solar energy is converted into electrical energy. During daytime the solar power supplies the needed power for the electrical equipment on board and the electric motor(s) as well as the power needed to charge the batteries for the night operation.

- Electric motor module
  Here the electrical energy is converted into mechanical energy.

- Energy storage system
  This could be normal batteries like Lithium-ion batteries, fuel cells or super capacitors or any hybrid system out of the mentioned (e.g. Lithium-ion batteries and super capacitors). [12] [69]

Well known representatives of solar powered HALE aircrafts are for example Pathfinder, Centurion, Helios, Global Hawk, Zephyr and SolarImpulse. [26] [52] [4]

2.1.1 Structure

For the solar powered aircraft it is most favorable to have a light structure so that the power needed to provide a stable flight is reduced, while supporting the needed technical equipment on board. It is common that the wings of these aircrafts are very large, or have a high aspect ratio (=ratio of the wing's length squared to the wing's area), so the weight is distributed along the wings. This is called span loaded airframe structure. If the aspect ratio, respectively the wing area, is greater, lift will be higher and drag will be lower. The drag is also lower because of the lower air density at these heights. The wings are also the places for the solar panels. Due to its large span (=length of the wing) and lightweight, the wing structure is very flexible. That is why the stability of the aircraft needs of course to be guaranteed. Therefore bending and tensile strengths need to be within the material limits. [37] [52] [30]

2.1.2 Payload

Depending on the mission of the HALE aircraft it has a certain payload. This could be for example camera(s) for aerial observation or any other necessary electrical equipment for recording data, a communication system to provide the unmanned flight and since solar panels are used as energy source a maximum power tracking device is needed as well as a proper storage system. Also insulation, especially for the electrical devices, is necessary or even a heating system, e.g. to hold a certain needed temperature to provide a good operating environment for the battery system, among other things. [26] [57]
Since the aircraft discussed in this paper shall replace satellites it also shall have the equipment a satellite would have. Therefore, five major components are needed: [5] [44] [39]

- EPS (**E**lectronic **P**ower **S**ubsystem)
  The EPS is responsible for delivering the necessary energy in form of voltage and current for the aircraft. Therefore, the aircraft has solar panels and an energy storage system.

- AOCS (**A**ttitude and **O**rbit **C**ontrol **S**ubsystem)
  The AOCS determines the position and navigates the aircraft to the desired position during the whole mission.

- OBDH (**O**n **B**oard **D**ata **H**andling)
  The OBDH is a kind of host computer which navigates and controls all the processes on board.

- RFS (**R**adio **F**requency **S**ubsystem)
  The RFS is the receiving and sender unit of the aircraft. Here the aircraft can send and receive data to and from the ground control.

- TCS (**T**hermal **C**ontrol **S**ubsystem)
  The TCE is responsible for regulating the temperature of the aircraft. Since it can be pretty cold and also quite hot (sunny side) in these altitudes and the electronic as well as the mechanical components

work better or just at certain temperature ranges, insulation and even heating systems are necessary to provide a good flight.

2.1.3 Applications

In former times these aircrafts were designed for military applications but recently there is a large potential for civil purposes. A HALE aircraft could be used for surveillance in general, atmospheric monitoring, supporting tactical battlefield operations, precise agricultural/wild fire monitoring, landscape mapping as well as any other mission which requires satellite-based infrastructure of a high-definition imagery. These aircrafts can also replace satellites in the same areas where satellites are used nowadays like for research, communication or military purpose. Satellites are very expensive and they have their own orbit around the earth. HALE aircrafts do not need to stay on a stated path around the earth and are cheaper than satellites. So if you want to make photographs for mapping a certain area on earth a HALE aircraft could be sent there as often you want and could circle the area of interest as long as necessary, but a satellite can only take pictures when it is orbiting above the particular spot. So with a HALE aircraft you can have these certain data quicker. [18] [12]

2.2 Solar cells

2.2.1 Thin film solar panels

The solar cells fixed on the wings of the aircraft convert the solar energy from the sun into electricity. The aircraft is powered by solar cells and batteries. During daytime the solar cells generate power which is needed to fly at maximum altitude and also to charge the batteries for the night. Obtaining a sufficient flight, power goes hand in hand with selecting an appropriate photovoltaic (PV) system and taking efficiency as well as weight into consideration for a long endurance flight. The solar cells are "thin film"

cells so the thickness varies from a few nanometers to some micrometers. This is very practical because these cells are very light, flexible and have a low drag. The thin film solar cells are less efficient than the conventional solar panels. But they are cheaper and their high flexibility makes them a better choice for this applications. They can be bended like the wing form without causing damages and even offer a great performance in extreme environments. The wings are fixed elastically so they can swing and stretch depending on the load. The solar cells are also affected by that, so their high flexibility is a must. Three types of thin film solar panels are dominant on the market nowadays: amorphous silicon, cadmium telluride and copper indium gallium selenite. [38] [19]

- Cadmium telluride
  This is the predominate technology with an efficiency factor of 16.5 %. The costs for manufacturing are quite low but negative aspects are the rather medium efficiency and the highly toxic cadmium. The recycling is quite costly.

- Amorphous silicon
  These panels have an efficiency factor of 14.9 %, so rather low efficiency while the equipment costs are quite high. But the technology is quite well developed.

- Copper indium gallium selenite
  On one side the market share is not very high and the cells are very expensive in production. On the other side the efficiency is quiet high, 19.9 %, but compared to the other technologies these cells are developing slower, because the other two have already achieved a greater demand on the market thus they have yet been better developed.

The efficiency of solar cells, in general, depends on several environmental features and weather parameters like wind speed, humidity, temperature, sun intensity and so on. For extraterrestrial purpose the amorphous silicon cells are common due to their high flexibility. These cells weigh around 100

$\frac{g}{m^2}$. On this field also the copper indium gallium selenite cells will play a bigger role in the future because of their good efficiency and flexibility.
In this paper amorphous silicon cells are used as energy supplier. [8] [1]

2.2.2 Maximum power point tracker (MPPT)

The generated power during the flight mostly depends on temperature, time of the day, the inclination of the cells with respect to the sun and the load current. During the flight the radiation intensity and hence the power output from the cells is not monotonic due to the unpredictable nature of the solar energy. Additionally, the output voltage is very low due to the small available area for the solar panels. Nevertheless all the electrical devices on the plane demand energy. To satisfy these demands as well as considering the unpredictability and uncertainties of the solar energy a MPPT is necessary. This device keeps current and voltage working for maximum power disregarding any changes in load or other conditions (e.g. changes in the atmosphere) and also optimizes the utilization of the PV cells. [20]

2.3 Energy storage

Energy storage is very important for the HALE aircraft. It needs to store energy for the night flight. Rechargeable batteries are energy storage devices which can convert the chemical energy into electrical energy and vice versa. The batteries mostly used nowadays are Lithium-ion batteries and took around 40% up to 70% of the total weight of the aircraft. By replacing this battery system by fuel cells or combinations with super capacitors, the weight can be reduced. In this paper Lithium-ion batteries, proton exchange membrane fuel cells (PEMFC or PEM), solid oxide fuel cells (SOFC) and super capacitors (SC) are in focus.
In the following paragraphs the lifetimes and their limitations and the actually used batteries as well as the possible substitutes (PEM, SOFC, SC) are described in general. [42]

2.3.1 Lifetime

A main challenge for a wider usage of batteries in mobile applications is their limited lifetime and the associated costs. A (charge) cycle of a battery is characterized as charging a rechargeable battery and discharging it as required into a load. Several external factors influence the lifetime negatively like overheating, coldness, overcharging or deep discharge. Overcharging is when the battery is still charged even when it has already reached its maximum charge. This causes the damage of the battery when it happens frequently. Deep discharge could also lead to the battery's early death. When the battery is discharged under 5% of the energy stored in the battery frequently this leads to a faster death of the battery (around 500 cycles). Complete discharge leads to an even faster battery breakdown (around 300 cycles). Deep discharge also causes a longer charging time and could lead to overheating of the battery while charging. Overheating and coldness have a negative influence on the chemical reactions in the battery. Keeping the battery within its operating temperatures guarantees better operation and larger lifetime. Also the lifetime in theory and the lifetime in reality differ a lot. The best developed technology described in this paper is the Lithium-ion battery. [16] In theory, the lifetime of this battery type is set to

- 10 – 15 years when the battery undergoes a cycle once per week and
- 4 – 7 years when the battery undergoes a cycle once per day.

The lifetimes of proton exchange membrane fuel cells, solid oxide fuel cells and super capacitors are dependent on three things:

- Electrolyte life
  If the electrolyte is a solid it will basically never go bad. If it is a fluid which will evaporate and eventually cause the fuel cell or super capacitor to fail.
- Voltage Derating
  Using a fuel cell or super capacitor at close to its maximum, voltage will cause it to fail more quickly than using it at a lower voltage. This tradeoff is known as a derating curve.

- Temperature
  Especially, the PEMFC and the capacitor are negatively affected by heat. It causes the electrolyte to evaporate more quickly, causes the dielectric to be weakened, and it can damage the thin conducting elements (the membrane in PEMFC). Both environmental heat and self-heating effects should be considered. [60] [34]

For PEMFC the lifetime varies from 3 – 5 years when charging and discharging every day. The lifetime of SOFC varies from 4 – 5 years. A super capacitor could have a lifetime up to 12 – 15 years. These lifetimes are just provided in theory. In reality several of the already mentioned factors have a greater impact, since the operation does not take place under the best possible conditions. The best possible conditions could just be provided in a laboratory. [29] [35]

2.3.2 Battery in general

Batteries are an interconnection of several similar galvanic cells. An electric cell is an electrochemical energy storage system and energy converter. While discharging the stored chemical energy is converted into electrical energy and thus can supply an electrical load independent of the grid.
A battery consists of three phases: anode, cathode and a separator. [64]

2.3.3 Lithium-based batteries

Nowadays Lithium-based batteries are used to store the surplus of solar energy in solar powered aircrafts. One big obstacle is that these batteries are pretty heavy, minimum 40% of the total weight. Since the trend tends to light weight HALE aircrafts to save energy there is lot of room for improvement. [62] [33]
In Lithium-ion batteries all three phases are Lithium compounds. Lithium-ion batteries are thermal stable and only suffer a minor Memory effect. [36] Memory effect occurs when rechargeable batteries are not fully discharged

between charge cycles and they remember the shortened cycle and are thus reduced in capacity (length of use per charge). You can also store these batteries a longer time because of its low self-discharging. These batteries also have a high specific energy density: compared to Nickel-Cadmium batteries it can store 3 to 4 times the energy amount. [14]
The most important advantages in summary are:

- high energy density
- high voltage
- low self-discharge rate
- wide temperature range in operation

These batteries are very vulnerable to deep discharging or overcharging. When the battery is always deep discharged the lifetime of the battery is pretty low, but when discharging down to 10% the best lifetime is fund. Another disadvantage is the relative high sensibility for too high or too low temperatures. The best working range for these batteries lies between +5 °C to +35 °C, but there are special Lithium-ion accumulators which can be used for very low temperatures down to −50 °C and still provide enough power. But for the flight altitude a HALE aircraft operates, the temperature can go down to −80 °C at night. So there the battery system suffers at these cold temperatures. A heating system would be a good solution to keep the batteries at their optimum operating temperature. The energy which would be needed to heat the battery system is smaller than the energy which would be wasted without the heating supply.
So the most important disadvantages are:

- long charging time
- poor cycle performance

- poor safety characteristics

Recently, also Lithium-sulphur batteries are used as energy storage system. This battery type provides higher energy density than the Lithium-ion battery. The compounds next to Lithium, Sulphur and Carbon, are cheap, common and easily available. But a problem is the charging cycles: the lifetime of this battery type is quiet low nowadays. [62] [46]
In this paper for the original model the commonly used Lithium-ion batteries are chosen.

2.3.4 Fuel cells

While internal combustion engines change chemical energy of (fossil) fuel to thermal energy to generate mechanical and/or electrical energy, fuel cells convert chemical energy from fuel directly into electrical energy. This direct conversion promises power generation with a high efficiency factor because fuel cells are not determined by thermodynamic limitations of heat engines such as the Carnot efficiency. Low environmental impact is possible by avoiding combustion and the accompanying generation of carbon dioxide (CO_2). If provided a constant source of fuel and oxygen to sustain the chemical reactions, fuel cells can (theoretically) produce electricity indefinitely.
The structure of a fuel cell is similar to the structure of a battery. It consists of three parts: anode, cathode and an electrolyte. The basic principle, that the cell works, is the reaction between hydrogen and oxygen. In every fuel cell type you have a material delivering the H^+, the donor (anode), and these protons are wandering through the electrolyte to the acceptor (cathode) and react with the oxidant, e.g. oxygen. The efficiency of fuel cells is quiet high, the product of the process is water and there are no pollutant emissions. Great obstacles are the high investment costs and the short lifetime.
Most work to date has focused on using fuel cells as battery replacements on small Unmanned Aerial Vehicles (UAVs). For this paper two types of fuel cells are discussed: the proton exchange membrane fuel cell, operating at low

temperatures, and in recent times the solid oxide fuel cell, operating at high temperatures. Proton exchange membrane, also called polymer electrolyte membrane, fuel cells and solid oxide fuel cells are two of the most developed types of fuel cells. In recent years lots of research was done for this fuel cells as energy sources.
Fuel cells offer a promising technology for clean, efficient power generation which is important for high altitude long endurance (HALE) remotely piloted aircrafts. Fuel cells can be used as exclusive energy source but also in combination with normal batteries or super capacitors. These possibilities are discussed under chapter 4. [41] [27]
Fuel cells are used in mobile or stationary applications. The fuel cell system could be an open or closed cycle (or loop) system. In an open cycle fuel cell system the produced and by-passed gases are not stored. In a closed cycle fuel cell system the produced and most of the by-passed gases are stored and used as gas supply. For the use of fuel cells in the HALE aircraft closed a cycle fuel cell system is necessary. In a closed cycle fuel cell system the reactants are regenerated by an auxiliary process, such as electrolysis. In a closed cycle no extra tank for the fuel need to be placed in the aircraft because an electrolyzer provides the needed fuel. The electrolysis is the inverse process of the process in a fuel cell.
A simple example to show the processes in a fuel cell and in an electrolyzer:

- fuel cell

  $2 \cdot H^+ + O^{2-} \rightarrow H_2O$ (waste)

- electrolyzer

  $H_2O \rightarrow 2 \cdot H^+ + O^{2-}$ (regenerated reactants)

2.3.4.1 Proton Exchange Membrane fuel cell (PEMFC)

Because of major investments especially by the automotive industry over the past decade, PEM fuel cell technology is at a relatively high state of

development. PEM fuel cells typically use pure hydrogen (H_2) as fuel. Hydrogen fuel is channeled through field flow plates to the anode, while the oxidant (oxygen or just air) is channeled to the cathode. At the anode, a platinum (or similar material) catalyst causes the hydrogen to split into positively charged H^+-ions (protons) and negatively charged electrons. The polymer electrolyte membrane (PEM) allows only the positively charged ions to pass through it to the cathode. The electrons migrate out of the electrolyte and through a wire that connects the anode to move towards the cathode, producing an electric current. At the cathode, the electrons and the H^+-ions combine with the oxygen to form water, which flows out of the cell as waste. Relatively low operating temperatures (80 °C) make PEM fuel cells an attractive option. Proton exchange membrane fuel cells are made possible by polymer electrolyte membranes. These membranes are composed of a solid, organic polymer that must be hydrated in order for the H^+-ions to be mobile. Therefore, PEM fuel cells must be operated under conditions that maintain liquid water. A humidity above 80% is favorable to guarantee good operation. Today's PEM fuel cell systems achieve efficiencies between 40 and 70%. [35] [60]

2.3.4.2 Solid Oxide fuel cell (SOFC)

In SOFCs, the electrolyte is a solid oxide or ceramic. A solid oxide electrolyte transports oxygen ions (O^{2-}) rather than H^+-ions. At the cathode, O_2 from air is reduced to O^{2-} and the O^{2-}-ions are transported through the electrolyte to the anode. At the anode, O^{2-}-ions react with gaseous fuel to produce water and heat and release electrons to the external circuit. It is not obligatory to use pure H_2; the reactions are not compromised by any byproduct and these byproducts just leave the fuel cell as waste: because the electrolyte transports O^{2-}-ions rather than H^+-ions, SOFCs can oxidize hydrocarbons and do not require pure H_2 as fuel. Typical operating temperatures of SOFCs range from 650 to 1000 °C. These high temperatures are driven in part by the choice of electrolyte. Because of its properties as a good O^{2-}-ion conductor and a stable electrolyte, yttria-stabilized zirconia (YSZ) is a popular electrolyte

with operating temperatures over 700 °C. These temperatures remove the need for catalysts in many cases because electrochemical reactions proceed more quickly at higher temperatures. Efficiency of SOFCs ranges from 40 to 65%. [64] [35]

2.3.5 Super capacitors (SC)

Super capacitors are electrochemical capacitors and so a further development of double layer capacitors. You can divide the capacitors into three main families:

- Double layer capacitors
  The electrodes are made of carbon (or a derivate) and have a very high static double layer capacity. The amount of faradaic pseudo-capacity is quite low.

- Pseudo-capacitors
  The electrodes are made of metal oxides or conducting polymers and have a very high pseudo-capacity.

- Hybrid-capacitors
  They have asymmetric electrodes, one with high double layer capacity and one with high pseudo-capacity.

Compared to accumulators of same weight the super capacitors have a quite low energy density but the power density is very high. This leads to a very fast charging and discharging ability and they also have more charging cycles than accumulators, hence a longer lifetime. Super capacitors are ideal for energy storage that undergoes frequent charge and discharge cycles at high current and short duration. [11]
The modern super capacitor is not a battery per se but crosses the boundary into battery technology by using special electrodes and electrolyte. In this paper the double layer capacitors (DLC) are in focus. DLCs are carbon-based with an organic electrolyte that is easy to manufacture. Today DLCs are the most common system in use. Super capacitors work well as low-maintenance

memory backup to bridge short power interruptions, rather than operating as a stand-alone energy storage device. The charge time of a super capacitor is about 10 seconds. The initial charge can be made very fast, and the topping charge will take some extra time. The super capacitor cannot go into overcharge; the current simply stops flowing when the capacitor is full. Provision must be made to limit the initial current inrush when charging a completely empty super capacitor. The super capacitor can be charged and discharged virtually an unlimited number of times. Also ageing has no influence on the device. Under normal conditions, a super capacitor fades from the original 100% capacity to 80% in 12 – 15 years. The super capacitor functions well at hot and cold temperatures. [16]
The self-discharge of a super capacitor is higher than in electrochemical battery. The stored energy of a super capacitor decreases from 100 to 50% in about a month. A battery discharges 10 to 15% at the same time. But the self-discharge rates of the different energy storage devices is not an issue in this paper. The focus is the time while the aircraft is flying and not resting. So during flight the self-discharge of the energy storage devices has no influence on the energy storage system.
On the one hand super capacitors are expensive in terms of cost per watt. But on the other hand they are lighter and so weight is saved, and thus less energy is needed for flying. [66] [29]

2.3.6 Gravitational potential energy

Gravitational potential energy is the potential energy stored in an object as a result of its height. When reducing the height this energy is partly released. This is important during night flight because there is just minimum or no solar energy available. So by reducing the height saves energy which the aircraft would need during the night. So not that much energy needed to be stored in the installed energy storage system to come through the night. So either the storage system could have a smaller scale, and thus weight could be saved, or deep discharging could be prevented for the actual energy storage

system and its lifetime would increase. [70]

2.4 Environmental constraints

During the day the aircraft flies at is maximum possible height, and loading its batteries with the surplus of solar energy. But during night, while running off batteries, the height decreases to save energy. Batteries contribute a lot to the overall weight, about 40% and higher. Thus a possibility to save weight would be to lower altitude and take advantage of the potential energy. With lower altitudes the atmosphere is denser, the wind speeds are smaller, but the drag is increasing. From former flight excursions is known that with increasing drag the power needed at lower altitudes is also increasing.
Cold temperatures, cosmic rays and the low pressures and lower density at the flight level have certain effects on the airplane components.
Air pressure ranges from about 1000 mbar at sea level to 50 mbar at the normal flight altitude of this aircraft. The same goes for the temperature range: 40 °C at sea level and about −80 °C during the night at the higher altitudes (15 – 20 km).
The air density is lower in higher altitudes, thus less air is there to build winds to shake the aircraft but the aircraft needs air to move forward. So on the one hand less air leads to lower resistance but on the other hand it leads to lower propulsion. If the aircraft flies at lower altitudes the air density is thicker, moving forward is easier, but also there occur more often more harmful storms or winds which could harm the aircraft or change its flight course.
The HALE aircraft normally flies at altitudes around 15 – 20 km, which means it flies in the zone where the troposphere meets the stratosphere. This area is also the area where the temperature reaches pretty low levels (around −80 °C at night). Therefore, the electronic or other sensitive equipment on board of the airplane is vulnerable for failures. So there need to be special arrangements (e.g. insulation, additional heating system(s)) that there occur as little malfunctions as possible during the flight. [52] [6]
In this flight altitudes also cosmic rays should be considered. Cosmic rays

are energetic particles, mostly protons, which interact with molecules in the atmosphere (e.g. oxygen). These particles lead to a faster altering of the aircraft's electrical equipment. Hence, flying at these high altitudes leads to special requirements like using special fibers and wires material and maintenance with increasing regularity. The altering effect appear after 4 – 6 months of constantly flying at these altitudes (15 – 20 km). [47] [3]
Since the missions for the HALE aircraft described in this thesis shall last 24 hours up to a few days, this is not an issue.

Chapter 3

Sizing the aircraft

In this chapter a snapshot of a typical modern HALE aircraft is shown. Some estimated values and other data from literature help to make a proper model of a HALE aircraft for further validation. First, estimations about the general structure of the aircraft are made, followed by making estimations about the energy storage and solar cell system. After that, the weight and stability of the aircraft can be determined.

3.1 General description of the aircraft

In this paragraph important definitions are explained and estimations about the sizes of the aircraft's body and wings are made. Also the drag forces and powers and the lift forces and powers are calculated. These information are used to design the energy storage and solar cell system. Also an estimation about the possible lifetime of the battery system is given as well as an overall mass statement.

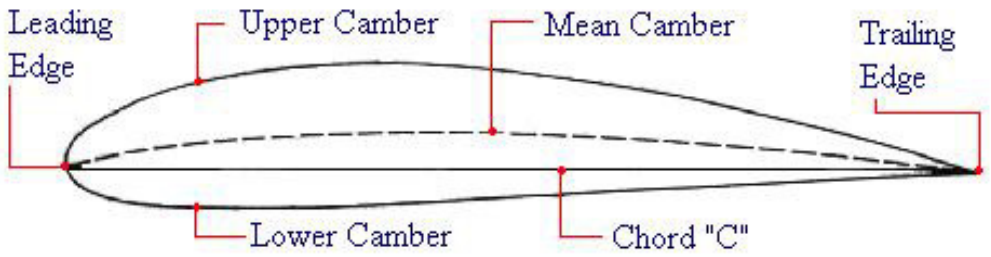

Figure 1: Airfoil description [49]; Important terminologies of an airfoil are shown here. The description of these terminologies is given in this chapter.

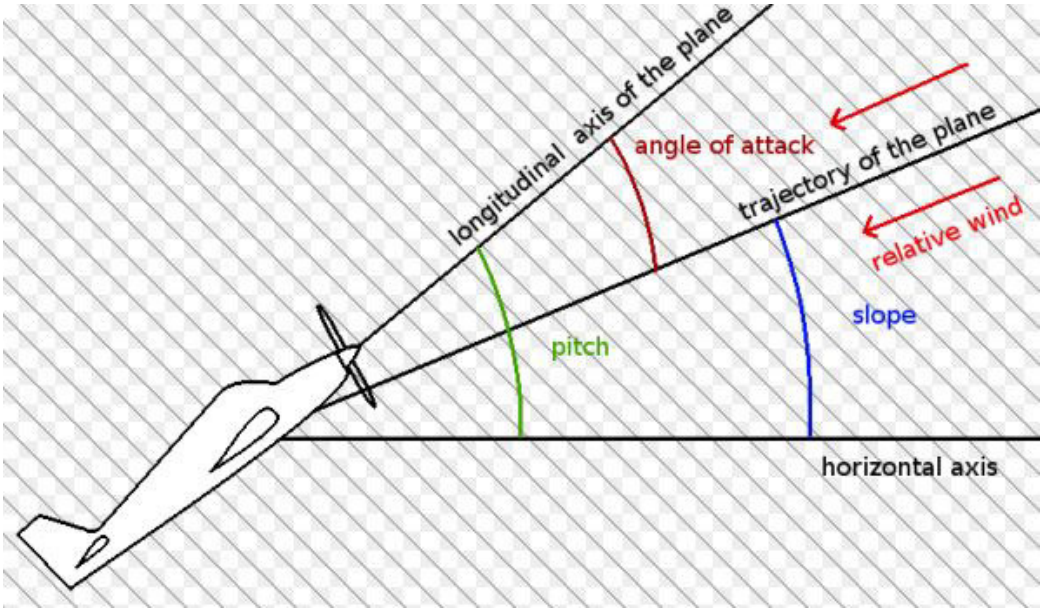

Figure 2: Angle of attack, slope and pitch [61]; Angle of attack, slope and pitch of an aircraft are shown graphically here. The description of these terminologies is given next.

The most important terminologies are: [56] [31] [59]

- Aerodynamic Center
  The point on the chord line about which the moment coefficient c_m is constant with changes in angle of attack (AoA). It is also the point where all changes to lift effectively occur.

- Angle of Attack (AoA)
  The angle of attack (AoA) is the angle between the trajectory and the longitudinal axis of the aircraft. The angle of attack has been a key aeronautical-engineering parameter and is fundamental to understand many aspects of airplane performance, stability, and control. (see figure 2)

- Slope
  The angle of climb (slope) is the angle between the horizontal axis and the aircraft flight path. (see figure 2)

- Pitch
  The pitch is the angle between the horizontal axis and the longitudinal axis of the aircraft. (see figure 2)

- Leading edge
  Forward edge of the airfoil (see figure 1)

- Trailing edge
  Aft edge of the airfoil (see figure 1)

- Span s
  The wing's length is called span.

- Chord c
  The wing's depth (or breadth) is called chord. (see figure 1)

- Aspect ratio (AR)
  The aspect ratio of a wing is the ratio of the span to its chord (special case: wing is a rectangle) or the span squared to the wing's area (for every wing shape)

- Center of Pressure
  The point along the chord line through which all aerodynamic forces (lift, drag, weight and thrust) act.

- Chord Line
  A straight line that connects the leading edge and the trailing edge of an airfoil. (see figure 1 Chord "C")

- Camber
  Camber is the term for the asymmetry between an airfoil's upper and lower side. Camber is designed to increase the maximum lift coefficient. This minimizes the stalling speed of an aircraft using a cambered airfoil. In general, a curved wing is more efficient than a flat wing: air moves cleanly over the top, which causes lower pressure to develop with less drag. (see figure 1)

- Camber line
  The camber line of an airfoil shape is a line drawn through the center of the airfoil (it is equidistant from the top and bottom surfaces), from the leading to trailing edge. So a fat, high-lift airfoil has a more curved camber line. A thin, high-speed airfoil has a flatter curve. The more curved the camber line, the more lift a given surface will generate. (see figure 1)

- Drag Coefficient, c_d
  A non-dimensional way of expressing drag which is independent of size and velocity.

  $\rightarrow c_d = \frac{2 \cdot F_d}{\rho \cdot v^2 \cdot A}$, where F_d is the drag force [N], A is the reference area $[m^2]$, ρ is the density $[\frac{kg}{m^3}]$ and v stands for the speed $[\frac{m}{s}]$.

- Lift Coefficient, c_l
  A non-dimensional way of expressing lift which is independent of size and velocity. It is primarily a function of AoA.

$\rightarrow c_l = \frac{F_l}{\rho \cdot v^2 \cdot A_{planform}}$, where F_l is the lift force [N], $A_{planform}$ is the planform (projected) area $[m^2]$, ρ is the density $[\frac{kg}{m^3}]$ and v stands for the speed $[\frac{m}{s}]$.

- Pitching moment coefficient c_m
  Pitching moment coefficient c_m is fundamental for defining the aerodynamic center of an airfoil. The aerodynamic center is defined to be the point on the chord line of the airfoil at which the pitching moment coefficient does not vary with angle of attack or at least does not vary significantly.

  $\rightarrow c_m = \frac{M}{\rho \cdot v^2 \cdot A_{planform} \cdot c}$, where M is the pitching moment [Nm], $A_{planform}$ is the planform (projected) area $[m^2]$, ρ is the density $[\frac{kg}{m^3}]$, v stands for the speed $[\frac{m}{s}]$ and c for the chord [m].

- Flight Path Velocity
  The speed and direction of the airfoil as it passes through the atmosphere.

- Relative Wind
  Air in motion with respect to an airfoil. It is equal to and in the opposite direction of the flight path velocity of an airfoil.

- Mach Number (Ma)
  The ratio of the velocity of a body to that of sound in the surrounding medium. The Mach number depends on the condition of the surrounding medium, in particular pressure and temperature.
  $\rightarrow Ma = \frac{v}{c}$, where v is the speed of the aircraft and c the speed of sound.

- Reynolds number (Re)
  As an aircraft (or any other object) moves through atmosphere, the

molecules (gas) of the atmosphere around it are disturbed and move around the object. Aerodynamic forces are generated between the molecules and the object. Aerodynamic forces depend in a complex way on the viscosity of the gas. As an aircraft moves through, the gas molecules stick to the surface of the aircraft. This creates a layer of air near the surface, a boundary layer, which slightly changes the shape of the object. The Reynolds number is a dimensionless number. Re, the non-dimensional velocity, can be defined as the ratio of

- the inertia force (ρ [$\frac{kg}{m^3}$], v [$\frac{m}{s}$], L [m]), and
- the viscous or friction force (μ [$\frac{N \cdot s}{m^2}$])

$\rightarrow Re = \frac{\rho \cdot v \cdot L}{\mu}$

High values of the parameter (the order of 10^6) indicate that viscous forces are small and the flow is essentially inviscid.

- Dihedral
  The span wise inclination of a wing or other surface such as a stabilizer.
- Glide ratio E
  The glide ratio $E = \frac{max \ \ c_l}{max \ \ c_d}$ shows how long an aircraft glide by losing 1 m in height.

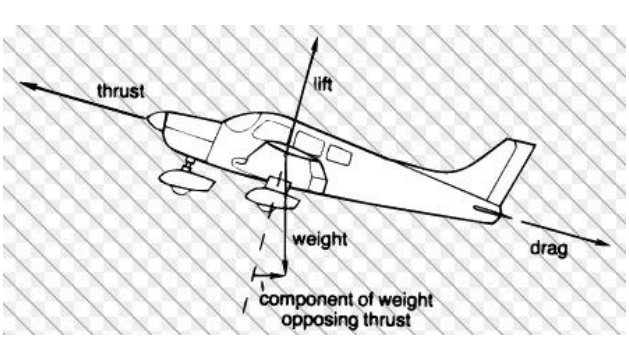

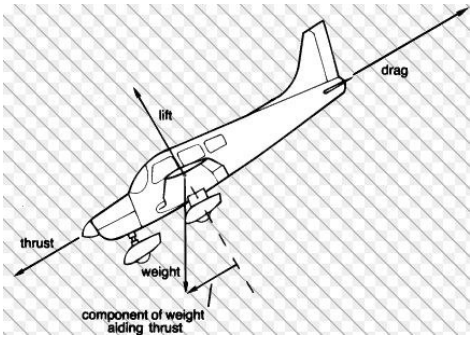

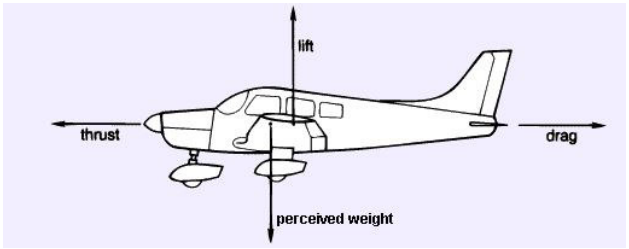

The classic four forces during flight are shown during normal flight (left, next to this text), in a climb (left, upper picture row) and in a descent (right, upper picture row).

Figure 3: Four aerodynamic of flight [45]

In general, four aerodynamic forces act on an aircraft: thrust, drag, lift and weight. [23] [24]

- Thrust T:
  Forward force produced by the propeller. It opposes or overcomes the drag force. So thrust is a mechanical force generated by the engines to push the aircraft forward.

- Drag:
  Rearward, retarding force caused by the disruption of airflow by the wing, fuselage and other protruding objects.

  - Parasite Drag:
    Includes all the drag which is not directly related to the production of lift. It is generated by those areas of the airplane which disrupt the otherwise streamlined flow of air. This includes

parts protruding into the airflow such as the landing gear, rough surfaces, and the mixing of the air such as where the wing and the fuselage meet. With increasing airspeed of an aircraft, parasite drag also increases.

- Induced Drag:
  A direct byproduct of lift. It is greatest at slow speeds with a high angle of attack. Conversely, at higher speeds and at a lower angle of attack, induced drag decreases. If the two drag curves are combined and the values added together, there is a point at which drag is at the minimum. This point is known as $(\frac{Lift}{Drag})_{max}$ which is where lift compared to drag is at its greatest.

- Weight W:
  Combined load of the aircraft itself and the cargo. Weight generally pulls the aircraft downward because of the force of gravity. It opposes lift and acts vertically downward through the aircraft's center of gravity.

- Lift
  This force opposes the force of weight and is produced by the dynamic effect of the air acting on the airfoil, and acts perpendicular to the flightpath through the center of lift.
  The lift could be controlled with

  - airspeed: if all other factors remain constant a doubling of the airspeed develops four times more lift.
  - Angle of attack: If all other factors remain constant, an greater AoA increases lift.

Some assumptions need to be made before the next calculations:

- The aircraft flies straight and level, maintaining constant altitude, through still air.
- The axis of the engine shall be aligned with the straight-ahead direction. Then drag is opposite to thrust and lift is opposite to weight.

In reality, it is not safe to assume that lift always matches weight, or thrust matches drag but it is a good estimation to avoid overweight or to see that the model does or does not work correctly.
The wings of an airplane are very important: the wing geometry is one of the chief factors affecting lift and drag. In figure 4 below a simplified wing planform is shown. Normally, the chord length varies along the span, but not necessarily.
But for simplification this rectangle form is the wing form used in this thesis.

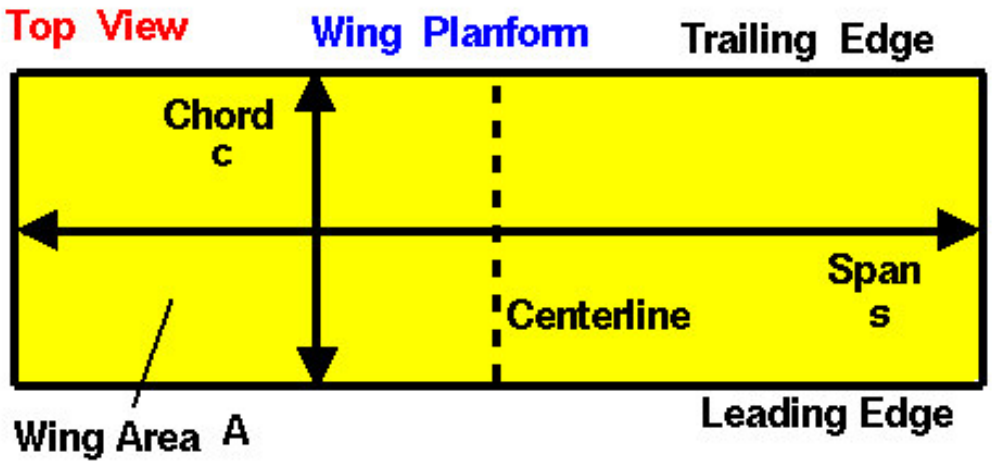

Figure 4: Wing schematic [2]; The wing shape and the important terminologies are shown. This figure is from the NASA website.

The aspect ratio of a wing is the ratio of the wing length (span) to its depth (chord) for the special case that the wing has a rectangular shape like here: $AR_{special\ case} = \frac{s}{c}$. For any other wing shape the aspect ratio has a more general form: the ratio of its span squared to the wing's area A: $AR = \frac{s^2}{A}$. A low aspect ratio indicates stubby and short wings whereas a high aspect ratio indicates long and narrow wings. Longer, narrow wings have less induced drag than shorter, wider wings. Induced drag is created at the tip of the wing, where the high pressure air from beneath the wing comes up over the wing tip into the low pressure zone. This meeting place of different air pressures becomes a turbulent area creating induced drag. The aspect ratio of a flying surface largely determines the lift to drag ratio of the

surface. A higher aspect ratio wing has a lower drag and a slightly higher lift than a lower aspect ratio wing. The span influences the drag negatively when it is too large, but the chord has no influence on the drag. [52] [40]
Good estimations for aspect ratios for HALE aircrafts vary from 12 – 25. For further calculations values for the span s and the chord c are set: a defined chord length of c = 1 m, a span length of s = 15 m. So the aspect ratio is AR = 15 and the wing area of one wing is $A = s \cdot c = 15\ m^2$.
The airframe structure is span loaded, which means the weight is distributed along the wings, and thus large wings are favorable. The wings also carry the solar panels which are needed to supply the power needed to fly.
The body of the aircraft shall have a cylindrical shape, for simplification, with radius r = 1.5 m, and length l = 9 m. These values are chosen from literature to match with the estimated wing size.
Next an appropriate airfoil need to be evaluated. The airfoil shall be E214. This airfoil is described as a popular glider airfoil. It has been already used on unmanned aerial vehicles (UAV). It is a high lift airfoil with relatively low drag. [63]
In figure 5 the form of the airfoil E214 is shown. It has a nonsymmetrical shape. This leads to better lift and lower drag than a symmetrically shaped airfoil. A nonsymmetrical airfoil has different upper and lower surfaces, with greater curvature of the airfoil above the chord line than below. Thus the mean camber line and chord line are different. A nonsymmetrical airfoil design produces useful lift where the angle of attack equals zero. Figure 6 shows the lift and drag forces on an aircraft and on a wing. [53] [55] [43]

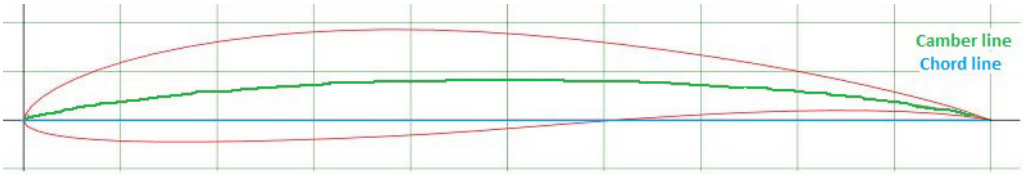

Figure 5: Airfoil E214 [63]; also the camber line and the chord line are shown.

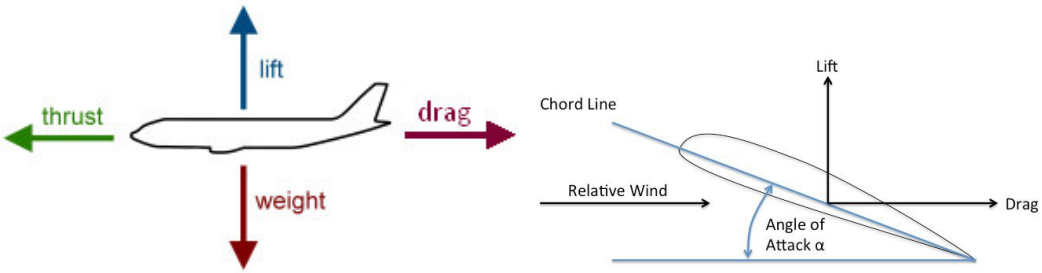

Figure 6: Aerodynamic forces on aircraft (left) and on the wing (right)

In table 1 important data of this airfoil E214 are listed. the development of these values is graphically shown in figures 7 to 12.

Table 1: Airfoil data, E214 [63]; here the most important airfoil data are shown. With this values for the best flight conditions are shown: the best angle of attack is 5°. The values from this table can be verified in the figures 7 to 10.

Maximum $\frac{F_l}{F_d}$	84.86
Maximum $\frac{F_l}{F_d}$ angle	5°
Thickness [%] (of chord)	11
Max. c_l	1.4178
Max. c_l angle	13°
Zero-lift angle	−4.5°
Camber	1.6°
Max. c_d	0.094
$E = \frac{max\ \ c_l}{max\ \ c_d}$	15.08

With the angle of attack (AoA), the coefficient of drag c_d, the coefficient of lift c_l and the pitching moment coefficient c_m the behavior of lift and drag can be described when changing the AoA or the pitch. In the graphics 7 to 12 this is shown.

In figure 7 the relation between the coefficients of lift and drag and their dependence on the different angles of attack is shown. Along the curve you see the different values for c_d and c_l for different angles of attack and with this values the best angles of attack and the corresponding coefficients for take-off, normal flight height and the landing can be determined. Also the minimum value for c_d, $c_{d,min} = 0.01011$, with the respective $AoA_{c_d,min} = -0.5°$ and the maximum value for c_l, $c_{l,max} = 1.4178$, with the respective $AoA_{c_l,max} = 13°$ are shown in this plot. When you draw a tangent from the zero point of the coordinate system to the polar line the best AoA for gliding is shown ($AoA_{gliding} = 5°$). The parable flight, where $c_l = 0$, is here defined with the zero-lift angle $AoA_{zerolift} = -4.5°$ and the respective $c_{d,0} = 0.01588$. The angle of attack has a range of $-8.5°$ to $17°$. An angle greater than $17°$ leads to stall and hence to a complete collapse of lift.

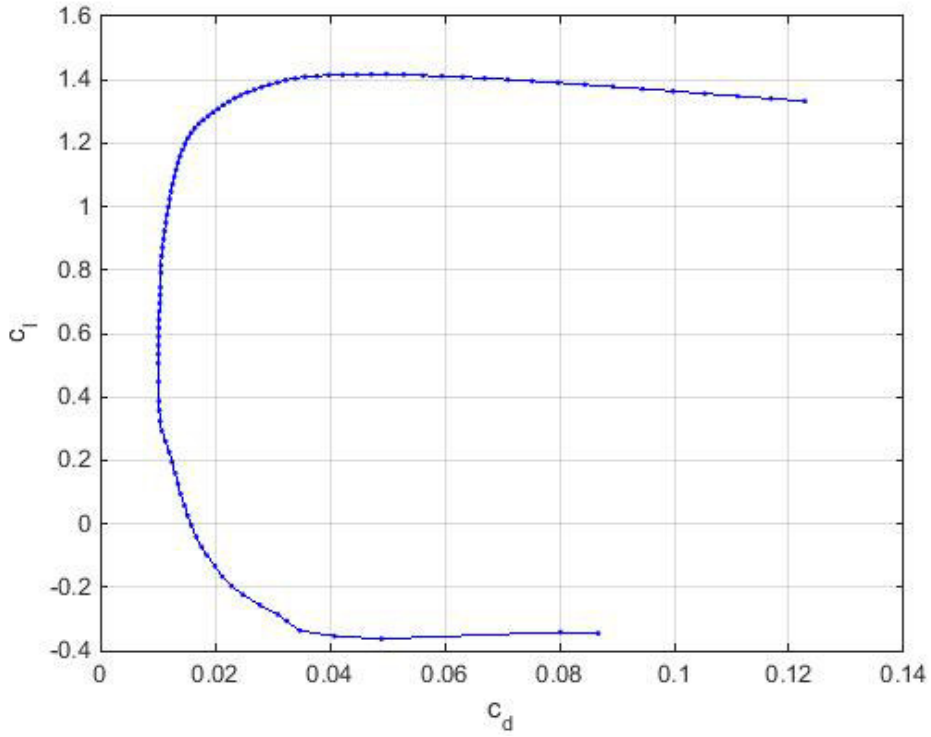

Figure 7: Polar diagram: Here the maximum and minimum values for the coefficients of drag c_d and lift c_l can be determined. Also different values for different glide ratios E can be determined.

The figures 8 and 9 help to determine these values more easily because there the lift or drag coefficient is shown in denpendence of the AoA. From these two figures the range for the best gliding can be determined with an as high as possible lift coefficient and an as low as possible drag coefficient: the best AoA range with high c_l would be from 0 to 13° and the best AoA range with low c_d would be from –3 to 7°, so the best AoA range for good horizontal flight shall be from 0 to 7° for this airfoil type.

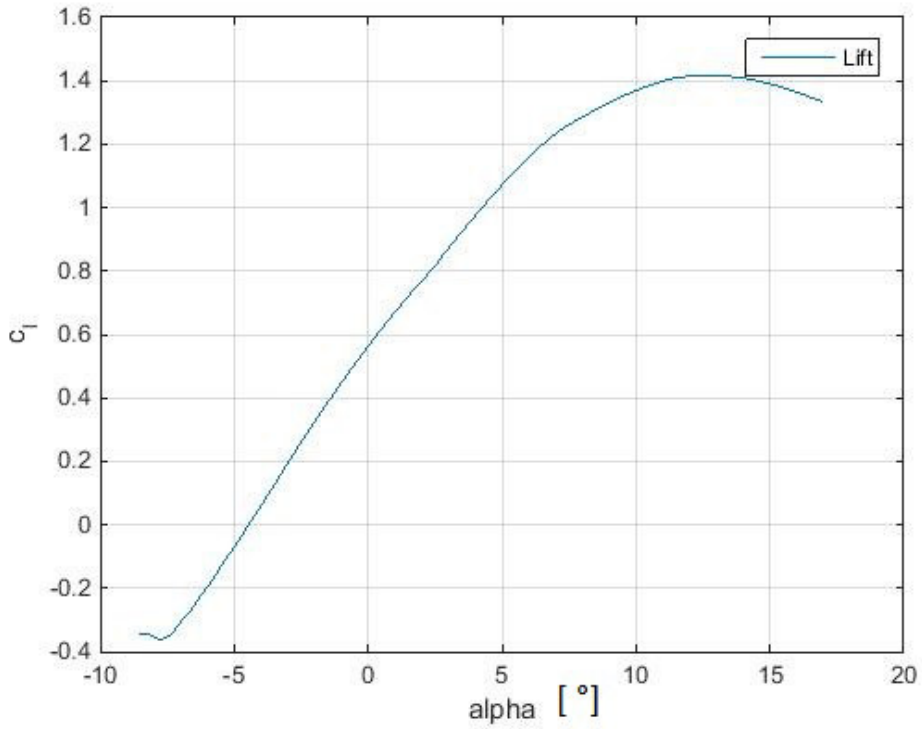

Figure 8: AoA vs c_l; Here the different angles of attack for the different values of the coefficients of lift c_l can be determined.

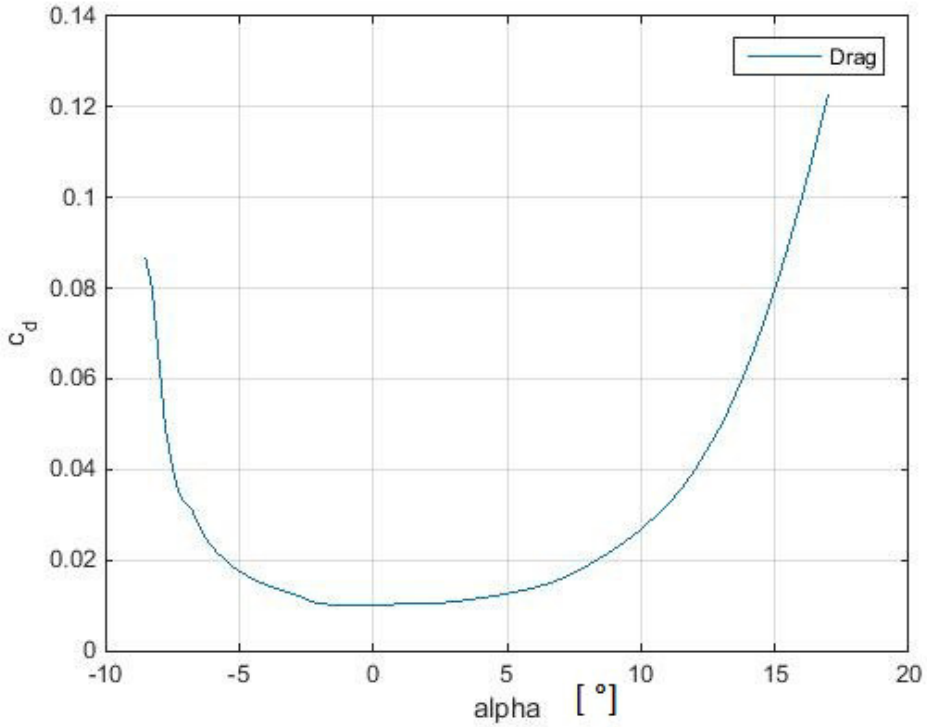

Figure 9: AoA vs c_d; Here the different angles of attack for the different values of the coefficients of drag c_d can be determined.

In figure 10 the $\frac{c_l}{c_d}$ ratio in dependence of the coefficient of lift c_l is shown. Along the curve the gliding ability of the aircraft is shown. At the maximum $\frac{c_l}{c_d}$ ratio the respective best lift coefficient is $c_l = 1.0709$ and drag coefficient is $c_d = 0.01262$. This values would provide the best horizontal flight. The best AoA would then be as mentioned 5° and lies perfectly within the best AoA range. The AoA range shall be 5° or lower, because there you would get better gliding ratios than having a bigger AoA than 5° because there the lift gets worse and worse until it collapses totally.

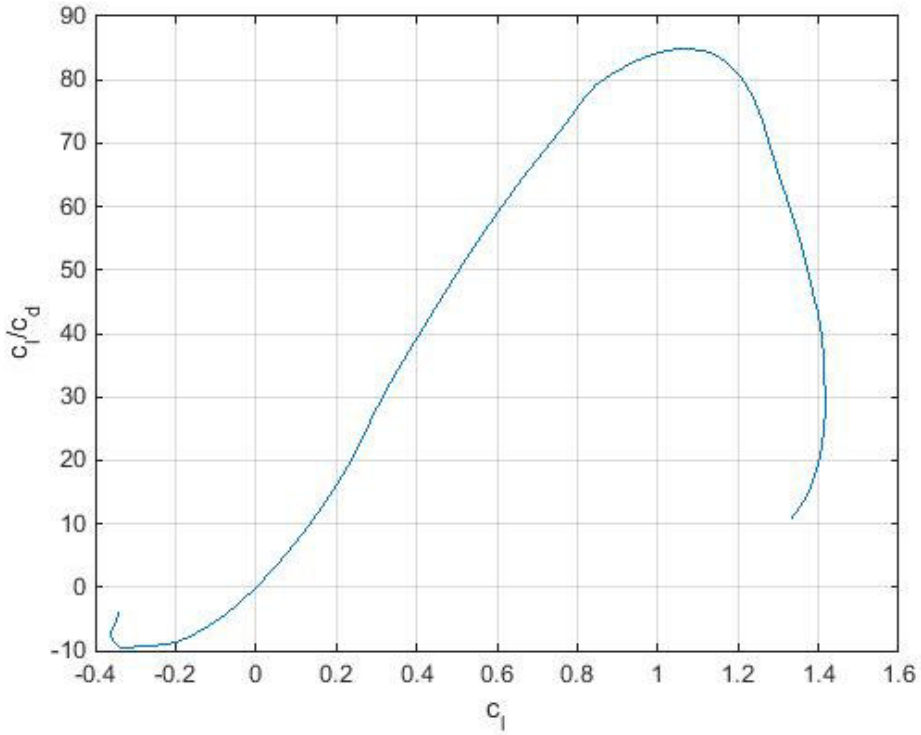

Figure 10: c_l vs c_l/c_d; Here the gliding ability is shown. The glide ratio increases until the maximum coefficient of lift c_l and then decreases drastically.

In figures 11 and 12 the relations between the lift coefficient c_l, respectively AoA, and pitching moment c_m are shown. The pitching moment coefficient c_m is important in the study of the longitudinal static stability of aircraft and missiles. The pitching moment coefficient is fundamental for defining of the aerodynamic center of an airfoil. For the minimum c_l the pitching moment c_m reaches its maximum. For medium c_l values (0.4 – 0.7) c_m reaches its minimum. The exact minimum of c_m can be determined in figure 12: For $\alpha = 0$ the minimum for c_m is $c_{m,min} = -0,1347$ and the corresponding value for c_l is $c_l = 0,563$. The backward movement of c_m for the highest values of c_l occurs because valid values for the pitching moment just occur until the best coefficient of lift $c_{l,max} = 1.4178$. Higher c_l values lead to a strange behaviour of the pitching moment (see also figure 12). But after the maximum value for $c_{l,max}$ (figure 11) or respectively the AoA at $AoA_{c_l,max} =$

13° (figure 12) the value for c_m gets lower until the stall and collapse of lift. The aerodynamic center is the point on the chord line of the airfoil at which the pitching moment coefficient does not vary with AoA or at least does not vary significantly over the operating range of AoA of the airfoil. The pitching moment is considered to be positive when it acts to pitch the airfoil in the nose-up direction. Conventional cambered airfoils supported at the aerodynamic center pitch nose-down, so the pitching moment coefficient of these airfoils is negative like in this paper.

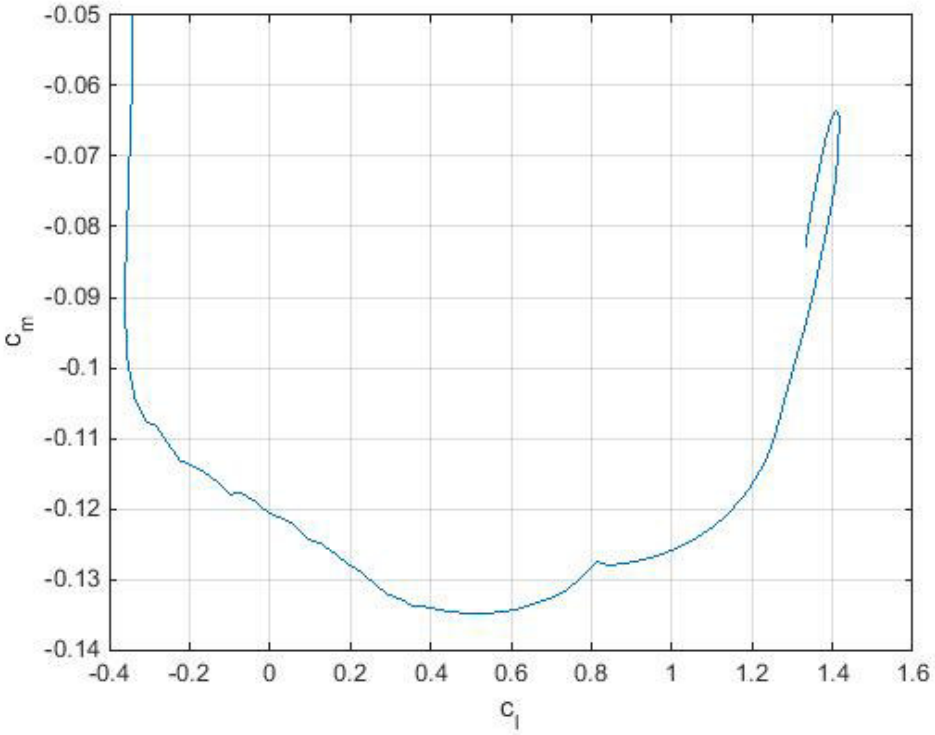

Figure 11: c_l vs c_m

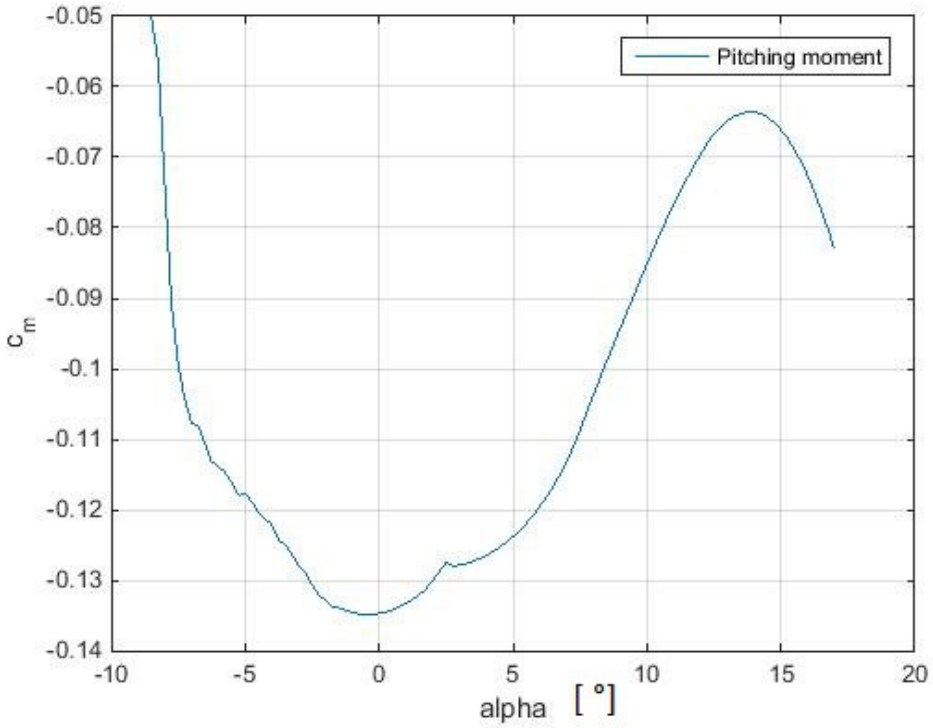

Figure 12: AoA vs c_m

The next step to determine the further aircraft structure and to find a valid propulsion system, is to calculate the drag and the lift. Therefore the density of the flight height and the velocity of the aircraft are important values. When air density decreases both, engine and aerodynamic performance, decrease. The reason is that with lower density air molecules are further apart from each other. A number of factors (altitude, pressure, temperature and humidity) have an influence on the air density. A higher altitude, low pressure area, lower temperature and high humidity all have one result: they lower the density of the air. And as a result of that: reduced aircraft performance. Density at the flight height is not the same as on earth, so the values need to be calculated with equation

$$\rho_h = \rho_{bottom,earth} \cdot e^{-\frac{h}{8400\ m}} \tag{3.1.1}$$

and the results for the different heights are shown in table 2. The density gets lower the higher the altitude gets. That is because in this heights there are less particles in the atmosphere, so there is more space for them to expand. Humidity is not an important factor at these altitudes that is why there are no data available. [7] [10]

Table 2: Density at higher altitudes; Here the altitude ranges from 15 to 20 km, which is the normal flight height of the HALE aircraft.

Height [m]	15,000	16,000	17,000	18,000	19,000	20,000
$\boldsymbol{\rho_h}$ $[\frac{\boldsymbol{kg}}{\boldsymbol{m^3}}]$	0.202	0.179	0.159	0.141	0.125	0.11

The dominating wind speeds in these heights are important: The wind varies greatly in speed and direction with change in seasons, being in general strong and westerly (25 to 50 $\frac{m}{s}$) during the winter, and light and easterly during the summer. For this paper the wind speeds are chosen around $v_{wind} = 180$ to $200\ \frac{km}{h} = 50$ to $55.6\ \frac{m}{s}$ – just 2% of the wind speeds are over this chosen range with maximum wind velocity values of $v_{wind,max} = 550\ \frac{km}{h} = 153\ \frac{m}{s}$ (winter season). In case this extreme values occur, the aircraft cannot fly against the wind but with the wind. The effective speed of the aircraft is $v = 20\ \frac{m}{s}$. So the speed range for the following calculations is $v_{min} = 50\ \frac{m}{s} - 20\ \frac{m}{s} = 30\ \frac{m}{s}$ and $v_{max} = 55.6\ \frac{m}{s} + 20\ \frac{m}{s} = 75.6\ \frac{m}{s}$.
Now that density and velocity are known, the drag and lift forces can be reckoned. Equation 3.1.2

$$F_d = c_d \cdot A \cdot \rho \cdot v^2 \tag{3.1.2}$$

is the formula for the drag force and the density at height h = 20 km $\rho_{20} = 0.11\ \frac{kg}{m^3}$ (table 2) is chosen. Equation 3.1.3

$$F_l = c_l \cdot A \cdot \rho \cdot v^2 \tag{3.1.3}$$

is the formula for calculating the lift force and, again the density at 20 km altitude is used. A stands for the area of interest (either wing or body of the aircraft). Not just at the wings parasite or induced drag occur but also on the fuselage. The body is described as a cylinder so the projected area is a rectangular solid with $r = 1.5\ m$ and $l = 9\ m$: $A_{fuselage} = 2 \cdot r \cdot l = 27\ m^2$. So for the forces acting on the aircraft's body this area need to be considered. The forces acting on the body are smaller than compared to the forces acting on the wings. The range between the minimum and the maximum forces respectively powers is enormous. That is because of the minimum and maximum speeds: the ratio between these two is big by squaring those (forces) and even bigger by cubing them (powers).
After the forces are known, the respective powers are calculated for the drag power

$$P_d = F_d \cdot v \tag{3.1.4}$$

and the lift power

$$P_l = F_l \cdot v_Z\ . \tag{3.1.5}$$

For calculating the lift power (see eqn. 3.1.5) the vertical component of the velocity v_Z is not known. Therefore, the time for the climbing up to a height of 20 km and the distance travelled until reaching the height of 20 km need to be determined. According to literature the following assumptions can be made:

- the distance for climbing shall be similar to the height $\Delta h = 20\ km$ (normally calculated with the Pythagoras' theorem)
- for the climbing time a median value from literature was chosen (22 min to climb up to $\Delta h = 20\ km$)

$\rightarrow$ The vertical velocity can be calculated with $v_Z = \frac{\Delta h}{t}$
Then the lift power could be determined. In table 3 the results for the

minimum and maximum drag and lift forces and powers are listed. Especially, the maximum power of drag (yellow marked) is important, because this number gives an outlook for the motor size. Here the engine needs to supply $\frac{330\ kW}{\eta_{Propulsion}}$ to supply a proper flight at 20 km altitude. But also the induced drag power and the power needed for the equipment, especially communication and heating, need to be taken into consideration to size the aircraft's engine properly. In the next step the induced drag is calculated. [63] [7]

Table 3: Results of the drag and lift forces and powers at 20 km altitude

	Minimum	**Maximum**
Velocity [$\frac{m}{s}$]	30	76
Drag force wings [N]	30	$2.3 \cdot 10^3$
Drag force body [N]	27	$2.1 \cdot 10^3$
Lift force wings [N]	$2.55 \cdot 10^3$	$1.96 \cdot 10^5$
Lift force body [N]	$2.29 \cdot 10^3$	$1.77 \cdot 10^5$
SUM drag force [N]	57	$4.4 \cdot 10^3$
SUM lift force [N]	$4.8 \cdot 10^3$	$3.7 \cdot 10^5$
Drag power wings [W]	900.8	$1.75 \cdot 10^5$
Drag power body [W]	810.7	$1.57 \cdot 10^5$
Lift power wings [W]	$7.64 \cdot 10^4$	$1.48 \cdot 10^7$
Lift power body [W]	$6.88 \cdot 10^4$	$1.33 \cdot 10^7$
SUM drag power [W]	$1.7 \cdot 10^3$	$3.3 \cdot 10^5$
SUM lift power [W]	$1.45 \cdot 10^5$	$2.81 \cdot 10^7$

For a three dimensional wing, there is an additional component of drag, called induced drag. The induced drag coefficient c_i

$$c_i = \frac{c_l^2}{\pi \cdot e \cdot AR} \tag{3.1.6}$$

is equal to the square of the lift coefficient c_l divided by pi times the aspect ratio AR times an efficiency factor e which describes the wing planform efficiency. Lowest induced drag occurs for an elliptic distribution of lift from tip to tip. The efficiency factor e is then equal to 1.0. So an elliptical wing planform has the lowest amount of induced drag and all other wing shapes have higher induced drag than an elliptical wing. For a rectangular wing, the efficiency factor is equal to 0.7 and with this factor the induced drag is calculated in this paper. The induced drag occurs not just on the wings but also on the fuselage of the aircraft. The induced drag force is calculated with equation

$$F_{Di} = c_i \cdot A \cdot \rho \cdot v^2 \tag{3.1.7}$$

and thereof the induced drag power with equation

$$P_{Di} = F_{Di} \cdot v \ . \tag{3.1.8}$$

In table 4 the induced drag powers P_{Di} are shown. The maximum induced drag power (marked yellow, table 4) is important and added to the value of the maximum drag power shown and marked yellow in table 3.

Table 4: Breakdown induced drag powers at 20 km altitude

	Minimum Drag power $P_{Di,min}$ [kW]	**Maximum Drag power $P_{Di,max}$ [kW]**	**S_i [m^2] (reference area)**
Wings	0.5	72.7	67.4
Fuselage	0.47	61	84.8
Sum	9.9	134	152.2

Next the propulsion system will be examined. Since the sum of the maximum drag powers (165 kW + 330 kW = 495 kW without additional weight and the efficiency factor of the propulsion system is not considered) is in a range of 500 kW – 1 MW, an engine category can be chosen. The motor shall be a DC motor powered by solar power at day and batteries at night. Chosen from a book of propulsion systems [25] an electric DC motor (ranges 400 kW up to 1 MW and voltage up to 2 kV) and a propeller were chosen with the efficiency factors $\eta_{Motor} = 0.92$ and $\eta_{Propeller} = 0.89$. So the overall efficiency of the propulsion system is $\eta_{Propulsion} = 0.82$. According to the tables in the book [25] this propulsion system weighs about 30 – 50 kg, including wiring and insulation.
First the needed power must be calculated (see eqn. 3.1.9). The power for the communication and heating systems is set to $P_{additional} = 350\ W$. The formula to calculate the needed power is

$$P_{needed} = \frac{P_{drag} + P_{induced\ drag}}{\eta_{Propulsion}} + P_{additional}\ . \tag{3.1.9}$$

The minimum needed power is $P_{needed,min} = 14.5\ kW$ and the maximum needed power is $P_{needed,max} = 566\ kW$, each defined as a sum minimum or maximum of parasite and induced drag. The maximum value for the needed power is more important for sizing the engines properly.

Next the thrust and weight shall be determined. A valid estimation for the thrust can be made with equation

$$\frac{F_l}{F_d} = \frac{F_W}{F_T};\ \frac{Lift}{Drag} = \frac{Weight}{Trust} \tag{3.1.10}$$

, because the trust need to overcome the drag. With the formula 3.1.10 the weight force F_W can be calculated. Then the maximum possible mass $m_{aircraft}$ of the aircraft can be calculated with equation

$$F_W = m_{aircraft} \cdot g\ . \tag{3.1.11}$$

This is important to see if the calculated total aircraft mass is within the limits (see paragraph 3.4).
In figures 13 and 14 the total drag force respectively the total drag power and its single components, induced and parasite drag, are shown. The lowest point in the total drag force curve corresponds to $v_{L/D}$, and gives the speed at the best lift-to-drag ratio. This occurs right at the point where the induced drag force curve crosses the parasite drag force curve. The lowest point in the curve for total drag power corresponds to the vertical speed v_Z and gives the best rate of climb. For this speed, in theory, the minimum shall occur right at the point where the parasite drag power is $\frac{3}{4}$th of the total, and the induced drag power is $\frac{1}{4}$th of the total drag power. Here in this case this speed occurs at the point where the parasite drag power is $\frac{2}{3}$rd of the total power and the induced drag power is $\frac{1}{3}$rd of the total drag power.

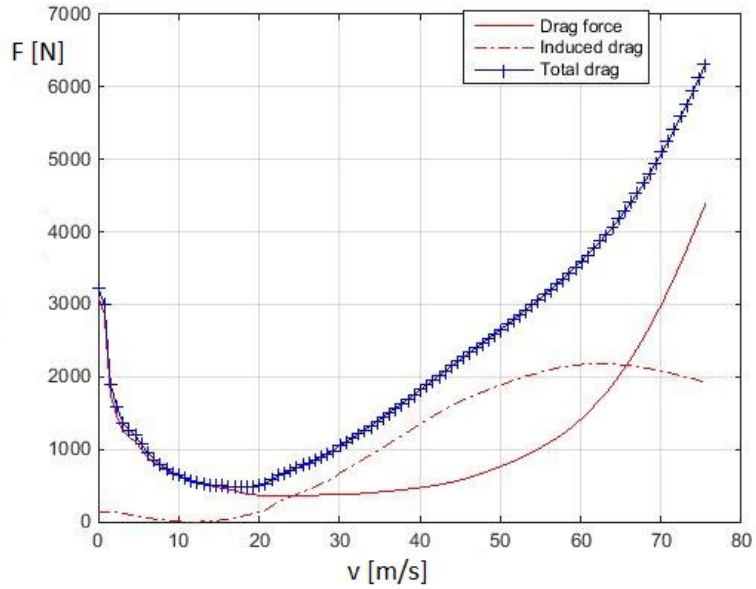

Figure 13: Drag forces; Induced and parasite drag forces are determined as well as the resulting drag force, all forces in dependence on the flight velocity.

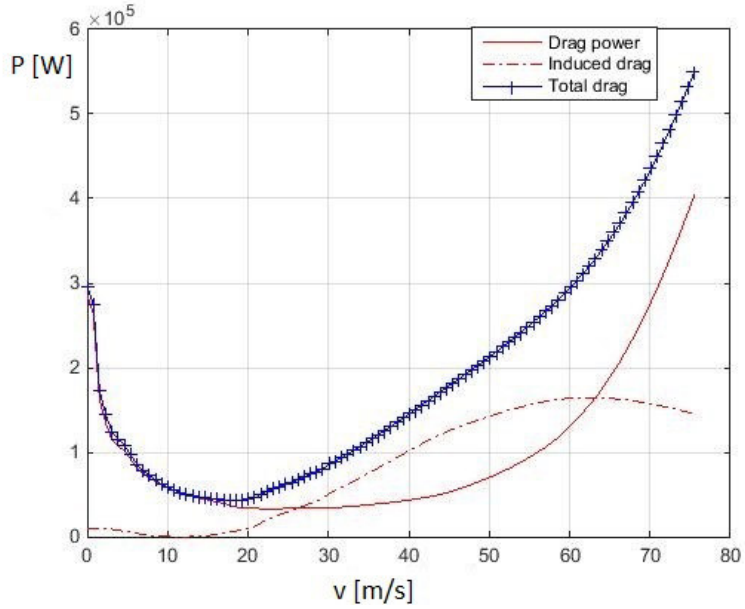

Figure 14: Drag power; Induced and parasite drag powers are determined as well as the resulting drag power, all powers in dependence on the flight velocity.

Excursus, altitude 30 km

Also considered is when the aircraft increase the height up to 30 km for a while. This could happen when the aircraft wants to get away from high clouds (equator) or extreme windy weather and the resulting turbulences at the present flight height. Here, just the maximum powers are calculated, because they are the most important. The maximum velocity is given with $v_{max,30} = 89\ \frac{m}{s}$, the cruising speed $v = 20\ \frac{m}{s}$ has already been added, and the appropriate air density is then $\rho_{30} = 0.033\ \frac{kg}{m^3}$ (see eqn. 3.1.1).
This climbing includes just the surplus added for the needed propulsion system so that it is not chosen too small. The extra power needed is $P_{30} = 214\ kW$ (maximum value see table 5, yellow marked cell). So adding this to the maximum needed power at 20 km the overall power would be $P_{needed,max} = 827\ kW$ (see eqn. 3.1.9).

Table 5: Power breakdown, 30 km altitude

	Maximum
Lift power wings [W]	$1 \cdot 10^6$
Lift power body [W]	$9.1 \cdot 10^5$
SUM Lift power [W]	$1.9 \cdot 10^6$
Drag power wings [W]	$8.7 \cdot 10^4$
Drag power body [W]	$7.8 \cdot 10^4$
SUM Drag power [W]	$1.65 \cdot 10^5$
Induced drag power wings [W]	$2.6 \cdot 10^4$
Induced drag power body [W]	$2.34 \cdot 10^4$
SUM induced drag power [W]	$4.94 \cdot 10^4$
TOTAL SUM drag power [W]	$2.14 \cdot 10^5$

In figure 15 the total drag power and its components are shown. Again, the

lowest point in the curve for total drag power corresponds to v_Z. For this speed the minimum shall occur right at the point where the parasite drag power: induced drag power is 3:1. Here in this case this speed occurs at the point where the parasite drag power is $\frac{3}{4}$th of the total power and the induced drag power is $\frac{1}{4}$th of the total drag power.
In figure 16 the total drag powers at 20 km and 30 km altitude are shown. Here you can see that the drag power is lower at higher altitudes. Also at 30 km altitude the drag power does not increase that fast at higher speeds in the given speed range. This could be explained with the fact that the respective coefficients c_d and c_i are dependent on the density and the density decreases with altitude all other variables stay almost the same. The wind speed is higher but in respect to the decrease in density the drag at 30 km altitude is smaller than at 20 km altitude.
At a speed of 60 $\frac{m}{s}$ and higher the drag powers increase faster than before. So in general are lower speeds favorable to keep the drag power lower.

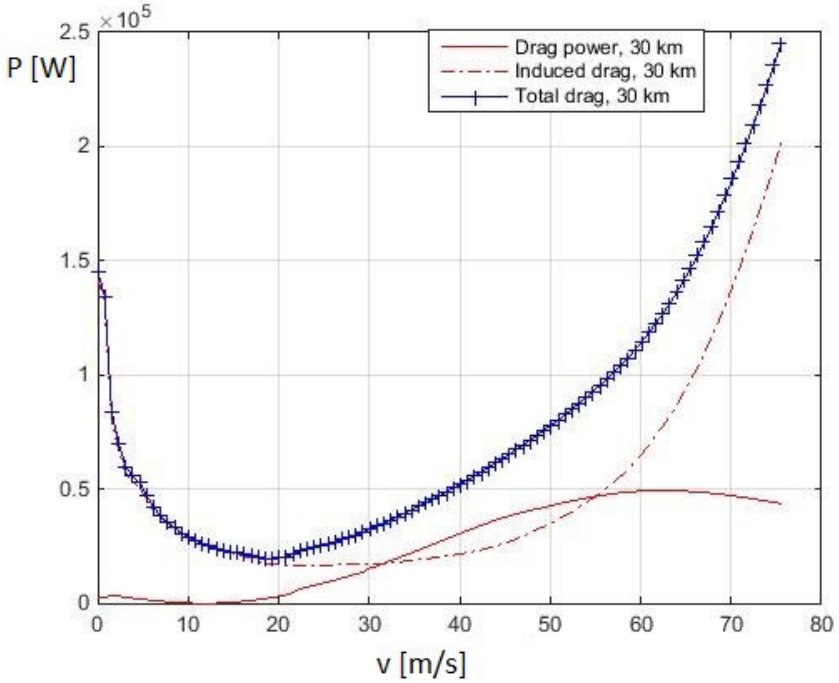

Figure 15: Drag powers at 30 km altitude in dependence on the flight velocity

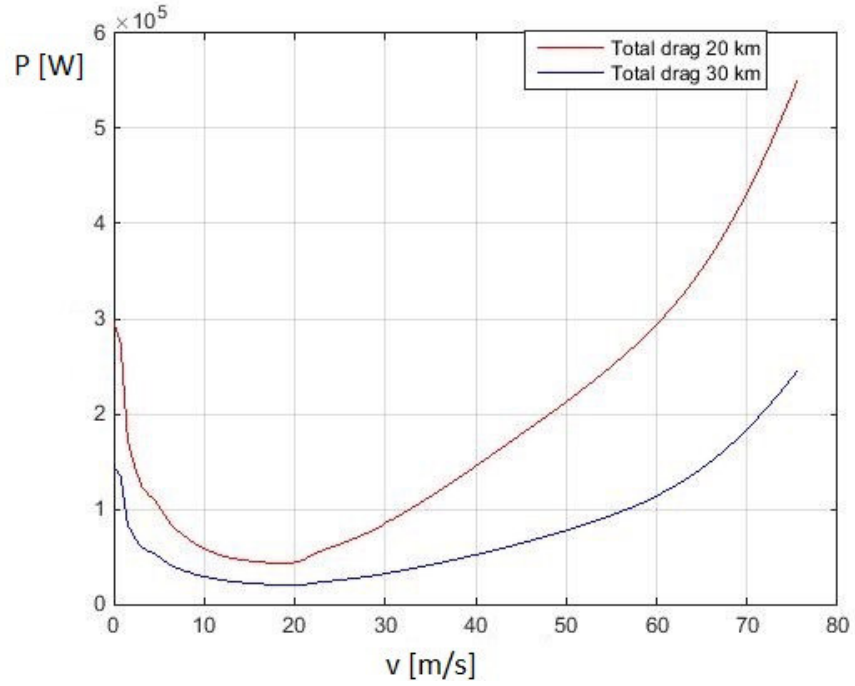

Figure 16: Drag powers - comparison 20 km and 30 km altitde in dependence on the flight velocity

From this present calculations an engine system is needed which supplies $P_{EL} = 600 - 850$ kW is necessary to provide a stable flight for the HALE aircraft in this paper. This could be supplied by an engine, located in the fuselage of the aircraft, and one propeller. Aircraft propellers convert rotary motion from electric motors to provide propulsive force to overcome the drag. The engine range which has been chosen before is valid here ($\eta_{Propulsion} = 0.82$, 2 kV). In the following paragraphs six different engine sizes are examined: 600 kW, 650 kW, 700 kW, 750 kW, 800 kW and 850 kW. With a 600 kW engine a stable flight at 20 km altitude is provided but the possibility to climb higher than this is next to impossible. With a 850 kW engine a stable flight at 20 km altitude as well as at 30 km altitude can be provided.

For the power for the engine a range between 600 to 850 kW is shown in the following calculations for solar panels and battery need. Also the possibilities and obstacles regarding the sunlight hours are shown.

3.2 Estimations: Solar power

In this thesis amorphous silicon cells are selected as energy supplier. In table 6 the data for the chosen solar panels are shown. These solar panels are very small but with high operating current and voltage. They are primarily used for special applications in aerospace because they are quite expensive. [69] [13]

Table 6: Thin-film solar cell data [13]

Property	**Solar panel**
Operating voltage V_{DC}	48 V
Operating current I_{DC}	12 A
Typical V_{OC}	49 V
Typical I_{SC}	16 A
Total size	100 mm x 50 mm
Thickness	0.04 mm
Weight	9.0 g

The P_{MPP} is the value for the maximum power of one solar panel given at the operating voltage and current (data for voltage and current from table 6). The P_{MPP} for the thin film solar cells used in this thesis is

$$P_{MPP} = V_{DC} \cdot I_{DC} = 576\ W\ . \tag{3.2.1}$$

The fill factor FF

$$Fill\ Factor\ FF = \frac{P_{MPP}}{V_{OC} \cdot I_{SC}} = 0.73 \tag{3.2.2}$$

describes the ratio between the maximum power and the value by multiplication

of open circuit voltage V_{OC} and short circuit current I_{SC}. This factor shows the quality of a solar cell. Here, the fill factor is FF = 0.73 (see eqn. 3.2.2), which is within the range of the FF for amorphous silicon: $FF_{amorphous\ silicon} = 0.6, ..., 0.75$. This shows that the used cells are upper level amorphous silicon solar cells and quite good.

The latitude plays an important role: The highest amount of global radiation is at the equator and decreases towards the poles. In this paper two latitudes are in focus: the equator, 0°, and a moderate latitude, 50°. The problem here is to get the right data for the solar irradiation at the flight height. According to literature appropriate data for solar radiation at heights of 16 – 23 km at latitudes 0° and 50° are listed in table 7. [51] [32] [9] [48]

With increasing altitude there is an increase in solar radiation. This increase is mainly due to an increase of direct irradiance, because there are less particles in the atmosphere which could scatter the radiation. So less solar cells need to be installed to get the same amount of power output as a similar solar power plant on earth. [3]

The length of a day, the sunshine hours, varies at least in moderate latitudes (see table 7). This plays a role in longer winter nights, when the battery system need to provide enough energy for a stable flight. [48]

The designing of the power supply shall be made for December, latitude 50°, because there are the worst conditions - less sun, hence less sun sunshine hours (see table 7) and solar power losses due to the sun's declination. To show all the possible scenarios the battery system need to be evaluated first (further calculations in chapter 3.3).

Table 7: Sun's Intensity at 50° latitude and at the equator [48] [52]

Month	**Intensity G, latitude 50°** $[\frac{W}{m^2}]$	**Intensity G, latitude 0°** $[\frac{W}{m^2}]$	**sunshine hours, latitude** 50°	**sunshine hours, latitude 0°**
Jan	98	248	7.5	12
Feb	140	247	9	12
Mar	168	232	10	12
Apr	200	251	12	12
May	206	250	14	12
Jun	243	247	15	12
Jul	270	250	16	12
Aug	245	249	14.5	12
Sept	230	261	13	12
Oct	188	268	11	12
Nov	123	252	9	12
Dec	88	310	7.5	12
	2199 $\frac{W}{m^2 a}$	2755 $\frac{W}{m^2 a}$		

According to the wing size and panel size 3,000 solar panels could be installed on each wing. This can be determined with the following three equations, where first the panels along the chord are calculated

$$Panels\ along\ chord = \frac{1\ m}{0.05\ m} = 20\ panels \tag{3.2.3}$$

and second the panels which can be installed along the span are determined with equation

$$Panels\ along\ span = \frac{15\ m}{0.1\ m} = 150\ panels\ . \tag{3.2.4}$$

With the results from these two equations the total amount of panels installed on one wing can be determined

$$Panels\ on\ one\ wing = 20 \cdot 250 = 3,000\ panels\ . \tag{3.2.5}$$

From equation

$$Minimum\ panels\ to\ install = \frac{600\ kW}{2 \cdot 576\ W} = 521\ panels,\ each\ wing \tag{3.2.6}$$

the minimum necessary amount of panels is calculated, for now with no regard on how the panels are wired: 521 panels on each wing are necessary to provide the power when the solar cells deliver the minimum needed power of 600 kW for powering the engines but the loading of the batteries for night is not possible here. The whole system is then scaled too small. In case the aircraft has just the minimum installed panels on the wings it has to follow the sun until its mission is over, but this is not a possible case here in this paper.
The panels are placed that the small panel side (50 mm) lies along the chord and the long panel side (100 mm) lies along the span, so the available space is used in the best way. So maximum 20 panels could be placed along chord and maximum 150 panels along span.
The area the solar cells cover on each wing are calculated with equation

$$Area\ solar\ cells,\ both\ wings = Number_{panels,wing} \cdot 2 \cdot A_{panel}\ . \tag{3.2.7}$$

The weight of the solar cells is important. Therefore, the number of installed panels times the weight of one solar cell, according to equation

$$Weight\ cells,\ both\ wings = Number_{panels,wing} \cdot 2 \cdot weight_{panel} \tag{3.2.8}$$

is calculated.
Also the wiring of the cells is important to find out how much cells can really be installed: according to the chosen electric motor an input of a voltage up to 2 kV is allowed. By wiring the panels in a row the voltage is added each time and the current stays the same. By wiring parallel the current is added each time and the voltage stays the same. The wiring shall be along the chord in row and along span parallel. This is implied in figure 17: the red line shows the wiring in a row along the chord and the green line shows the parallel wiring. By using maximum amount of cells the current for one wing would be $I = 150 \cdot 12\ A = 1800\ A$ and the voltage would be $V = 20 \cdot 48\ V = 960\ V$. Both, voltage and current, do not exceed the limits of the DC motor.

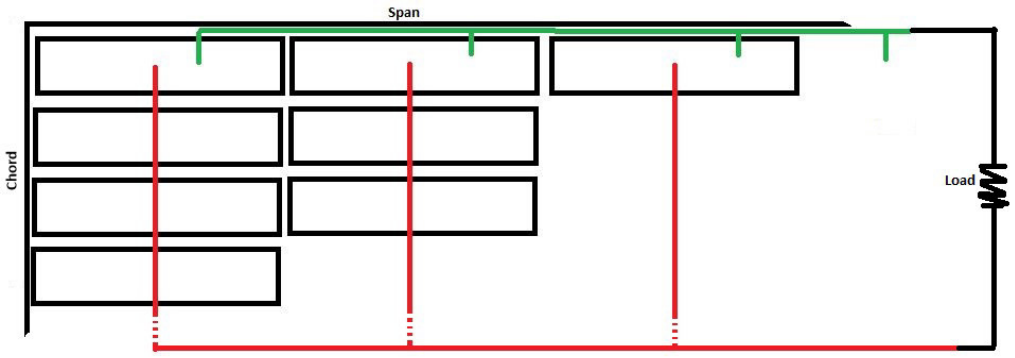

Figure 17: Wiring of the solar panels: The voltage is summed up when wiring in a row, the current is summed up when wiring parallel.

So the maximum available electrical power delivered from the solar panels is $P_{el,max} = 3.5\ MW$. Regarding worst case conditions only 70 – 75% of the

electrical power could be supplied: $P_{el,70} = 2.42\ MW$. The 25 – 30% power loss is defined as a 15% loss because of declination (December) and 8 – 15% loss because of shadowing because of the flight path. The flight path is best described as a circle or an eight over the area of interest. The loss because of declination and shadowing for every month is determined as followed:

- 30% loss in January, February, November and December → $P_{el,70}$
  15% loss because of declination and 15% loss because of shadowing
- 20% loss in March, April, September and October → $P_{el,80}$
  10% loss because of declination and 10% loss because of shadowing
- 15% loss in May, June, July and August → $P_{el,85}$
  5% loss because of declination and 8 – 10% loss because of shadowing

In figure 18 the change in panels along span and chord for different powers, respectively motor sizes, can be determined just by selecting a power and then drawing a horizontal line until it intersects with the chord and span curve. At the intersections a vertical line is drawn downwards and then from the x-axis the numbers of panels along span and chord are known. To get valid information a power between 600 – 850 kW or at least over 600 kW shall be chosen.

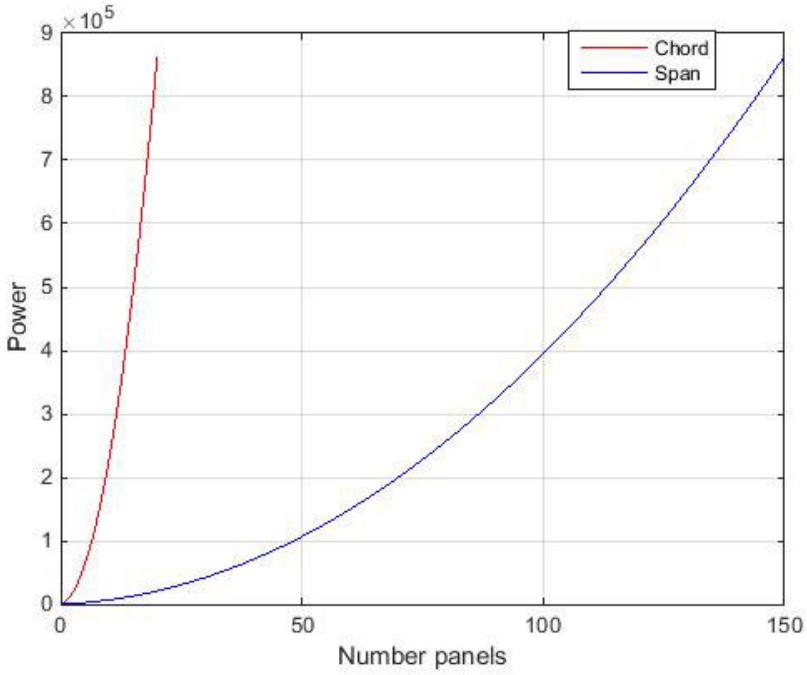

Figure 18: Panels: the change in panels along span and chord for different powers, respectively motor sizes, can be determined just by selecting a power and then drawing a horizontal line until it intersects with the chord and span curve. At the intersections a vertical line is drawn downwards and then from the x-axis the numbers of panels along span and chord are known.

Cloud cover has also an effect on the arriving amount of solar radiation. So called "high clouds" could reach the flight altitude when flying near the equator. For moderate latitudes there is no negative effect because of shading of clouds at the flying altitudes (see table 8).
The best way to get no problems with shadowing by clouds is just to raise the aircraft above the clouds. If this is not an option the percentage which is reflected or absorbed by the clouds does not exceed 25% (20% is reflected, when the clouds are very dense, and 3 – 5% is absorbed by the clouds) of the whole solar power. Since the loss because of declination does not exceed 5% at the equator and the solar radiation is higher than at moderate latitudes, the model which is determined for moderate latitudes is also valid when flying near the equator.

Table 8: International system, cloud classification [48]

Cloud family	**Moderate latitudes**	**Tropics**
High clouds	5 to 13 km	6 to 18 km
Middle high clouds	2 to 7 km	2 to 8 km
Deep clouds	0 to 2 km	0 to 2 km
Vertical clouds	0 to 3 km	0 to 3 km

The power demanded by the engine and the electrical systems and equipment of the aircraft could be supplied in two ways. The first option is that the solar cell system supplies the demanded power and then for this solar cell system the energy storage system is designed. The second option is that the needed power for the engine of the aircraft is supplied by the energy storage system and for this the solar cell system is designed.
It is better when the power for the engine is supplied by the battery system and then the solar cell system is designed for this storage system. A good reason for designing the battery system first is that during wintertime (January or December with 7.5 h of sunshine and 16.5 h of night, latitude 50°) the daytime is much shorter than the nighttime. This leads to less sunshine hours and hence less energy could be stored for the night then during summertime. So a greater battery system and a greater solar panel area is needed to provide a stable flight also during wintertime.
When designing first the solar panel system and then battery system the reference would be the month(s) with the most sunshine hours (July, 16 h of sunshine and 8 h of night, latitude 50°). So the solar panel area would also be quite big with a corresponding energy storage system. It could also be big enough for wintertime. But when there occur minor changes in environmental conditions to the worst during wintertime, the battery system could not supply enough for maintaining a stable flight at night. That is because the sunshine hours in July are less than the hours of night in winter (December/January) and with these values the system is defined. So it is better to supply the power the engine needs from the energy storage system and then design the solar system.

The final results could not be given without having a look at the battery system. In chapter 3.3 also panel's weight and the surface area they cover will be calculated, after the battery system is accurately defined.

3.3 Estimations: Battery system

The battery system used for the preliminary calculations, the "original system", is based on Lithium-ion batteries. In table 9 general information about Lithium-ion batteries are shown.

Table 9: Lithium-ion battery data [66]

Function	**Lithium-ion**
Charge time	10 – 60 min
Cycling (life time)	500 times and higher
Cell voltage	3.6 – 3.7 V
Specific energy $[\frac{Wh}{kg}]$	150 – 200
Specific power $[\frac{W}{kg}]$	1,000 – 3,000
Cost per Wh	$ 0.50 – $ 1.00
Charge temperature	0 – 45°C
Discharge temperature	-20 – 60°C

The efficiency of the battery system is set to $\eta_{battery} = 0.85$ for one cycle (charging and discharging once). Here a stack of batteries is used which consists of 100 batteries (25 in a row and 4 parallel) with the dimensions 500 x 240 x 62 (stack) and voltage V = 3.6 V and current I = 3.4 A for one battery. The weight for one stack is 0.95 kg.
The battery system is so designed that is supplies the power for the engine

and the range from 600 – 850 kW is taken into consideration. To calculate the corresponding solar cell system the sunshine hours from table 7 are needed. First, the energy which is needed overnight is calculated and then divided by the corresponding day hours to find out the power which shall be delivered by the solar cell system: $\frac{1}{T}\int E(t)dt$, while T stands for the sunshine hours and E for the energy, which needed to be stored in the energy storage system. The maximum power needed per month is calculated that way. In table 10 the real demand of solar power throughout the year is shown including the loss because of shadowing and declination. The yellow colored line shows the needed power from the solar cells under worst conditions. With the total amount of solar cells the needed power could be supplied.
The minimum power for worst conditions (December or January) demanded from the solar cells is 1.55 MW (engine size 1, table 10), so actually supplied shall be $\frac{1.55\ MW}{0.7} = 2.2\ MW$ because of the possibility that in worst case just 70% of the power could be supplied by the solar cells. Therefore, 1,920 panels are necessary on each wing: 15 panels along chord and 128 panels along span delivering the power demanded. With this just a flight (in wintertime) at 20 km altitude is possible. Including a possible increase in height up to 30 km engine size 6 is needed which means 2.2 MW (see table 10) coming from the solar cells. 2.2 MW are the worst case and equal 70% of the actual supplied power. The real power output coming from the solar cells is $\frac{2.2\ MW}{0.7} = 3.1\ MW$. Therefore, 2,698 panels on each wing are necessary: 19 panels along the chord and 142 panels along the span delivering the needed power. The weight for the installed solar power is $M_{solar} = 48.6\ kg$ instead of the maximum weight for solar power installed of $M_{solar,max} = 54\ kg$.
In table 10 also the needed batteries are shown and the corresponding weight as well as the volume of these battery system. This is important to know because the battery system shall be stored in the fuselage of the aircraft with $V_{fuselage} = \pi \cdot r^2 \cdot l = 63.6\ m^3$. According to this data there is no storage problem for the batteries.

Table 10: Real demand during the year

Engine size	1	2	3	4	5	6
Month	**600 kW**	**650 kW**	**700 kW**	**750 kW**	**800 kW**	**850 kW**
	[W] $10^6 \cdot$					
JAN	1.55	1.68	1.81	1.94	2.07	2.2
FEB	1.18	1.27	1.37	1.47	1.57	1.67
MAR	0.99	1.07	1.15	1.24	1.32	1.4
APR	0.71	0.76	0.82	0.88	0.94	1.0
MAY	0.5	0.55	0.59	0.63	0.67	0.71
JUN	0.42	0.46	0.49	0.53	0.56	0.6
JUL	0.35	0.38	0.41	0.44	0.47	0.5
AUG	0.46	0.50	0.54	0.58	0.62	0.66
SEPT	0.59	0.65	0.69	0.75	0.79	0.85
OCT	0.83	0.9	0.97	1.04	1.11	1.18
NOV	1.18	1.27	1.37	1.47	1.57	1.67
DEC	1.55	1.68	1.81	1.94	2.07	2.2
battery quantity	491	532	572	613	654	695
weight batteries [kg]	466	505	543	582	621	660
Volume $[m^3]$	3.65	3.96	4.26	4.56	4.87	5.17

A charge cycle is a process of charging a rechargeable battery and discharging it as required into a load. In table 11 the depth of discharge and the respective possible discharge cycles are shown. After the battery has reached the number of cycles stated in table 11 just 70 – 80% of the original capacity is left or the battery has already failed. A partial discharge reduces stress

and prolongs battery lifetime. Elevated temperature and high currents also have an effect on the lifetime.
Next an estimation about the battery lifetime is made. Therefore, an integral over the depth of discharge per month and a (median) value for discharge cycles (see 11) was calculated: during January and December the battery system is undergoing a deep discharge which means almost 100% of the stored power is used during night to provide a stable flight. So during these months the energy stored in potential energy could help to provide a stable flight. During February, March, October and November the battery system is discharged down to 10 – 20%. During April and September 30 – 35% of power is left in the batteries. From May until August 50 – 60% of power is left. With this information an estimation about the battery lifetime could be made: the battery system could last 1680 – 1845 cycles in best case. This is about 4 – 5 years since there is one cycle per day. The estimation is quite good because in literature the lifetime for Lithium-ion batteries, charging and discharging once per day, is set to 4 – 7 years.
To improve lifetime a possibility would be to install more batteries so that during January and December the batteries would not undergo deep discharge. But this has the negative side effect that the weight of the aircraft increases. This possibility is not taken into consideration in this paper.

Table 11: Lithium-ion battery discharge cycles [46]

Depth of discharge (DoD)	**Discharge cycles**
100 % (deep discharge)	300 – 500
50 %	1,200 – 1,500
25 %	2,000 – 2,500
10 %	3,750 – 4,700

3.4 Estimation: Weight and stability of the aircraft

The structure of the aircraft is made of ultra-light carbon fiber. Carbon fiber composite material has a general weight of 0.2 to 0.3 $\frac{kg}{m^2}$. In table 12 important properties of carbon fiber material are listed.

Table 12: Properties of Carbon fibre material [67]

Property	**Value**
Tensile strength σ_T	800 $\frac{N}{mm^2}$
Bending strength σ_B	1,000 $\frac{N}{mm^2}$
Density ρ	1,760 $\frac{kg}{m^3}$
Young's modulus E	230,000 $\frac{N}{mm^2}$

Next, the single masses of the aircraft are collected and evaluated. First the structure of the aircraft shall be determined by assuming that the wings are rectangular solids with chord:span:thickness 1:15:0.11, where the thickness equals the thickest part of the wing (see table 1). The surface area of a wing is approximately $S_{wing} = 33.5\ m^2$. The fuselage of the aircraft has a length of l = 9 m and a diameter of r = 1.5 m. The assumption for the surface area of the fuselage is a cylindrical form: $S_{fuselage} = 2 \cdot \pi \cdot r \cdot l = 2 \cdot \pi \cdot 1.5\ m \cdot 9\ m = 84.8\ m^2$. The total surface area is $S_{total} = 2 \cdot S_{wing} + S_{fuselage} = 151.9\ m^2$ and with the weight of the carbon fiber material $M_{ST} = 151.9\ m^2 \cdot 0.3\ \frac{kg}{m^2} = 45.6\ kg$. The weight for solar panels and batteries has already been calculated in previous paragraphs. The solutions are listed in table 13. In this table the maximum weight for the solar panels was added for all engine sizes. Since the contribution to the overall mass of the solar panel system is very small (maximum 54 kg), it is neglected in this mass statement. In chapter 4 more exact calculations are given and explained. The total mass M_{TOTAL} is determined for the six possible propulsion systems. The mass for the propulsion system, for the biggest engine, is estimated to be

$M_P = 50\ kg$. This value for the biggest propulsion system is added to every of the six engine sizes. The mass of the heating and communication systems and other important systems and equipment shall be $M_{SE} = 30\ kg$ and to be on the save side an additional weight of $M_{additional} = 50\ kg$ is added to the total weight. The weight for the aircraft's equipment and systems M_{SE} is hard to determine and depends on the mission the HALE aircraft has to fulfill. Here, the necessary five subsystems are included: Electronic power subsystem, attitude and orbit control subsystem, on board data handling, radio frequency subsystem and the thermal control subsystem. Depending on the mission e.g. different types of cameras are needed. Missions can also have a more complex purpose and so a special and/or more equipment is needed. Therefore the additional weight of 50 kg is added to the overall weight of the aircraft. The results are all overestimated since the weight for the biggest propulsion system, an additional weight and the weight for the maximum amount of solar cells is always added to the other masses. In the best case 30 – 40 kg could be subtracted from the overall aircraft mass. So it can be neglected here because the battery system contributes the most to the overall weight. In chapter 4 a more accurate mass statement is shown.

Table 13: Mass statement *

Engine size number		1	2	3	4	5	6
Engine	$P_{Propulsion}$	600 kW	650 kW	700 kW	750 kW	800 kW	850 kW
Total aircraft structure	M_{ST}	45.6 kg					
Propulsion system	M_P	50 kg					
Aircraft systems and equipment (communication and heating system, cameras, measurement and data control (...))	M_{SE}	30 kg (assumed: satellite)					
Solar panels max.	M_{Solar}	54 kg					
Battery system	M_{BS}	466 kg	505 kg	543 kg	582 kg	621 kg	660 kg
Extra assumption for additional things e.g. insulation	$M_{additional}$	50 kg (assumed: satellite)					
$\sum$ ***masses***	$\boldsymbol{M_{TOTAL}}$	696 kg	735 kg	773 kg	812 kg	851 kg	890 kg

* In this table the weights of the different propulsion systems are shown. The only thing changing the mass here, is the battery system consisting of Lithium-ion batteries. The maximum amount of solar panels is considered as well as the maximum weight for the propulsion system and the maximum weight for systems and equipment plus an additional weight.

Next the stability of the wings is tested: the tensile and bending strengths need to be within the limits (see table 12). Therefore, the deadweight and the solar panel weight forces are determined with equation $F = m \cdot g$, where m is the respective mass (solar cells, deadweight) and g is the gravitational acceleration and F is the resulting mass force. Normally these are distributed loads q(x) $[\frac{N}{m}]$ but for simplification the line loads are calculated with

$$F_R = \frac{q(x) \cdot L}{2} \ . \tag{3.4.1}$$

The resulting forces from the deadweight of the wing and the weight force of the installed solar panels are transformed into one resulting force $F_R = 628.4\ N$ with equation

$$F_R = F_{deadweight} + F_{solar} \ . \tag{3.4.2}$$

Then the moment is calculated with

$$M = \int_0^L q(x)dx \tag{3.4.3}$$

where L the length of the wing and the distributed line force q(x): $M = 4.7\ kNm$ (eqn. 3.4.3). Before the bending strength can be evaluated, the moment of inertia need to be calculated first with

$$I_y = \frac{a^3 \cdot b}{12} \tag{3.4.4}$$

for a rectangle: $I_y = 0.0017\ m^4$. Hence, the bending strength is calculated with this equation

$$\sigma_B = \frac{M \cdot L}{I_y} \ . \tag{3.4.5}$$

The result is $\sigma_B = 42.4\ \frac{N}{mm^2}$. The equation to calculate the tensile strength is

$$\sigma_T = \frac{F}{A} \tag{3.4.6}$$

and the result is $\sigma_T = 4.2 \cdot 10^{-5}\ \frac{N}{mm^2}$. Regarding table 12 the values are within the material's limit.

3.5 Estimation: Potential energy

Also the potential energy is important, because it is used during the night flight. The formula for calculating the potential energy for different height differences Δh is

$$E_{pot} = m_{total} \cdot \Delta h \cdot g\ . \tag{3.5.1}$$

In table 14 the gravitational potential is listed. At 20 km height the zero point is set because this shall be the normal flight height. Then $\Delta h = 1\ km, ..., \Delta h = 5\ km$ show the differences from 20 km when lowering the height until 15 km altitude is reached. $\Delta h = 10\ km$ shows the energy released when climbing down from 30 to 20 km. When climbing up to that height this amount has a negative influence on the power balance. The potential energy shall just be used at night to support the battery system. This could be important during the winter months. To get the corresponding power the night times are needed then the powers can be calculated for every month (see table 7). Since the worst scenario $\frac{2.2\ MW}{0.7} = 3.1\ MW$ (see table 10) need to be delivered from the solar panels and 695 battery stacks are needed to supply the 850 kW for the engine, climbing down to 15 km at night would save 4 battery stacks (saved energy in blue marked cell, see table 14), each stack carrying 100 batteries. Other way around, the same scenario ($\Delta h = 5\ km$, saved energy in blue marked cell, see table 14) but

this time in summer (July): now 18 battery stacks could be saved. But the battery stacks, which could be saved in summer are needed in wintertime. When descending from 30 to 20 km in December or January, 9 battery stacks could be saved (saved energy in purple marked cell, see table 14).
The saving in battery stacks is negligible because when going down from 20 to 15 km in winter time, not even 1% of battery stacks would be saved.

Table 14: Potential energy *

	$\Delta h =$ 0 m	$\Delta h =$ 1 m	$\Delta h =$ 2 m	$\Delta h =$ 3 m	$\Delta h =$ 4 m	$\Delta h =$ 5 m	$\Delta h =$ 10 m
	[Wh]	$10^4 \cdot$					
$M_{TOTAL,1}$	0	0.68	1.37	2.05	2.73	3.41	6.83
$M_{TOTAL,2}$	0	0.72	1.44	2.16	2.88	3.61	7.21
$M_{TOTAL,3}$	0	0.76	1.52	2.27	3.03	3.79	7.58
$M_{TOTAL,4}$	0	0.79	1.59	2.39	3.19	3.98	7.96
$M_{TOTAL,5}$	0	0.83	1.67	2.5	3.34	4.17	8.35
$M_{TOTAL,6}$	0	0.87	1.75	2.62	3.49	4.36	8.7

* In this table the potential energies for the different heights and the six aircraft masses for the six different propulsion systems are shown. $M_{TOTAL,1}$ represents the aircraft mass with engine size 600 kW. $M_{TOTAL,6}$ represents the aircraft's weight with engine size 850 kW. $M_{TOTAL,2}$ to $M_{TOTAL,5}$ represent the aircraft masses with the engine sizes 650 kW to 800 kW. The altitude of 20 km is here the reference point since this is defined as the normal flight height for HALE aircrafts.

Chapter 4

Implementing a new battery system

In this chapter a statement about the energy storage system is made. Therefore, the original system consisting of Lithium-ion batteries shall be replaced and hopefully the total aircraft's weight is reduced. The replacements are PEM and SO fuel cells and super capacitors. While the fuel cells can fully replace the existing battery system the super capacitors just act as partial substitute and are hence shown in various combinations with the Lithium-ion batteries, the PEMFC as well as the SOFC. Also the necessary amount of solar cells is shown and their weight is determined.
The PEM fuel cells are in a stack of 60 cells with stack dimensions of 256 mm x 115 mm x 75 mm. The weight of one stack is 1.4 kg and the efficiency shall be $\eta_{PEM} = 0.7$.
The solid oxide fuel cells are in a stack of 60 cells with dimensions of 360 mm x 180 mm x 65 mm. The weight of one stack is 5 kg and the efficiency is $\eta_{SOFC} = 0.65$. The SOFC has a higher weight and lower efficiency than the PEM fuel cell. Also for the SOFC a different heating system as well as a better insulation is needed because the operating temperatures are much higher than the operating temperatures for Lithium-ion batteries or the PEM fuel cells. When installing an improved heating system and better insulation the before estimated weight and power estimations do not exceed. Since

the aircraft's system and equipment mass was estimated high (30 kg, where the most important systems and equipment do not exceed 15 – 18 kg) and for worst cases an additional mass of 50 kg was added to the total aircraft mass. So the general constructed framework is still valid for SOFC. Later a breakdown of total weights and the tables in the next paragraphs show whether the SOFC could compete with the other options or not.
For both fuel cell types the efficiency factor was chosen very high, but this was on purpose since a good environment shall be made for the fuel cells to work under their best operating conditions. So the assumption of choosing these efficiencies is valid.
The equipment to provide a closed cycle fuel cell system (e.g. electrolyzer, pipes) has a weight of 10 – 12 kg. The efficiency of the electrolyzer is $\eta_{electrolyzer} = 0.45$. This weight was not counted extra since an overestimated mass for the systems and equipment and the additional mass already cover this extra weight.
The super capacitors are in a stack of 5 cells, plain, with dimensions of 30 mm x 30 mm x 5 mm and have an efficiency factor of $\eta_{SC} = 0.95$. The weight of the stack shall be 350 g. The super capacitors cannot replace the complete battery system but in parts. In theory it is possible to use just super capacitors but in reality the storage system would suffer under these conditions because of the constant use of the capacitor. It is more reliable for immediate supply for short term. 40 – 45% can be supplied by super capacitors without greater problems. But in not every case it is the best to partly substitute batteries or fuel cells with the most possible amount super capacitors. That depends on the energy storage system. This is explained later, also with help of table 16. The capacitors are not like the others placed in the fuselage, but along the underpart of the wings. In the following paragraphs the super capacitors support Lithium-ion batteries, PEMFC and SOFC with 20, 30 and 40% of the energy storage system. Even when 45% of the energy storage system could be substituted with super capacitors it is not shown here. But the trend or best choice of the substitution model is shown (see table 16).
In table 15 below a comparison between super capacitors and fuel cells is

given. The values are mean values regarding different manufacturers (also see table 9 to compare with the Lithium-ion batteries). The data from table 9 are added here to table 15 so the comparison is made easier between super capacitors, fuel cells and Lithium-ion batteries.
In table 15 the already discussed advantages and disadvantages of super capacitors, Lithium-ion batteries and the fuel cells are mentioned. As expected the super capacitor has a very fast charging time, low specific energy and high specific power compared to fuel cells and Lithium-ion batteries. There is no charging time for the fuel cells mentioned because they are not really charged. Since closed cycle fuel cell systems are used an extra application, an electrolyzer, provides the fuel. In an auxiliary process the reactants are regenerated. This recovery process happens simultaneously to the process in the fuel cells.
The values for the lifetime for the PEMFC (up to 9,000 h) and the SOFC (7,300 h) describe the lifetimes during a continuous operation until the fuel cells fail. So when the waste product (water, H_2O) from the fuel cells arrives in the electrolyzer, it is immediately transformed back into its single components (Hydrogen H_2 and oxygen O_2) and sent back to the fuel cells. So in theory both fuel cells can operate permanently for about one year: up to 375 days for PEMFC and 304 days for SOFC. It is possible to transform these values into cycles since the fuels cells do not work continuously, but just during the night. Therefore the operating hours (nighttime) of each day in each month are taken into account. The same estimation calculation like for the Lithium-ion battery lifetime in chapter 3 (paragraph 3) was made. In table 16 the solutions are listed.

Table 15: Performance comparison super capacitor / Fuel cell[66] [35] / Lithium-ion battery

Function	**Super capacitor**	**PEMFC**	**SOFC**	**Li-ion battery**
Charge time	1 – 10 s	————		10 – 60 min
Cycling (life time)	1 million times or 30,000 h	up to 9,000 h	7,300 h	500 times and higher
Cell voltage [V]	2.3 – 2.75	0.9	0.8	3.6 – 3.7
Specific energy [$\frac{Wh}{kg}$]	5 (typical number)	400 – 600	500	150 – 200
Specific power [$\frac{W}{kg}$]	up to 10,000	2,300	3,000	1,000 – 3,000
Cost per Wh [$]	20 (typical)	35	30 – 45	0.50 – 1.00
Operating temperature [°C]	-40 – 65	60 – 85	650 – 1000	-20 – 60

Regarding the lifetime of each of the systems an enormous improvement could be made when partly substituting the batteries or fuel cells by super capacitors. In table 16 the range of the possible lifetimes is shown for the different models. It is obvious that by partly sustituting batteries or fuel cells by super capacitors, the batteries, respectively the fuel cells, have a longer lifetime. Regarding the depths of discharge (DoD) over the whole year the medium discharge cycles for the models could be estimated. Therefore the same method which was already used to determine the lifetime of Lithium-ion batteries in paragraph 3.3 was used.
Looking at the models 1 – 3 (Original Li-ion, PEM and SOFC model) the best lifetime has the original model, hence the Lithium-ion batteries, followed by the PEM model. The worst lifetime here has the SOFC model, but the

differences in lifetime are not very big among the models. When substituting the energy storage system partly by super capacitors, then the lifetimes of all models rise. When replacing some batteries respectively fuel cells with super capacitors, the PEM/SC and the SOFC/SC models have greater lifetimes than the Li/SC models. So the partial replacement of batteries/fuel cells with super capacitors shows better lifetime results for the fuel cell/SC models than of the Li/SC models. Looking at the Li/SC models there is a great improvement in lifetime from the original model (4.6 years) to the Li 80%/SC 20% (5.5 years) model. Also from the Li 80%/SC 20% (5.5 years) to the Li 70%/SC 30% (6.5 years) the improvement in lifetime is steady and quite big, but the achievable improvement when installing Li 60%/SC 40% (6.9 years) instead of Li 70%/SC 30% (6.5 years) is lower. So there the fact of cost-benefit analysis, the trade-off, need to be determined to see if installing Li 60%/SC 40% (6.9 years) instead of Li 60%/SC 40% (6.5 years) is worth it. So if installing super capacitors (6 more super capacitors, see tables 20 and 21) instead of Lithium-ion batteries (70 battery stacks could be saved) is cheaper compared to the minor improvement in lifetime. Looking at the PEM/SC models an even greater improvement in lifetime was made when replacing fuel cells by super capacitors: from 4.5 years (PEM model) to 5.9 years (PEM 80%/SC 20% model). PEM 70%/SC 30% (6.7 years) and PEM 60%/SC 40% (7.5 years) models show steadily increasing lifetimes but a lower increase than from the PEM to the PEM 80%/SC 20% model. Also for the SOFC/SC models the trend goes like for the PEM/SC models: from SOFC (4.3 years) to the SOFC 80%/SC 20% (5.7 years) model the improvement is very big and for the SOFC 80%/SC 20% to the SOFC 70%/SC 30% and the SOFC 60%/SC 40% model the improvement is great. The best lifetime could be achieved with the PEM 60%/SC 40% model closely followed by SOFC 60%/SC 40% model and at last the Li 60%/SC 40% model. But looking at the best improvement from the models where just one type of energy storage system is used (Lithium-ion batteries, PEMFC or SOFC) and the models where 40% of the energy storage system is substituted by super capacitors, the SOFC 60%/SC 40% model achieved the greatest improvement.

These values exist just in theory and the preterm failures are not taken into account here.

Table 16: Discharging cycles for different models

	Model	**Cycles, min.**	**Years, min**	**Cycles, max.**	**Years, max**
1	Original	1680	4.6	1845	5
2	PEM	1650	4.5	1796	4.9
3	SOFC	1585	4.3	1754	4.8
4	PEM 80%, SC 20%	2150	5.9	2300	6.3
5	PEM 70%, SC 30%	2460	6.7	2520	6.9
6	PEM 60%, SC 40%	2720	7.5	2785	7.6
7	LI 80%, SC 20%	1995	5.5	2090	5.7
8	LI 70%, SC 30%	2290	6.5	2450	6.7
9	LI 60%, SC 40%	2620	6.9	2600	7.1
10	SOFC 80%, SC 20%	2090	5.7	2185	6
11	SOFC 70%, SC 30%	2305	6.3	2400	6.6
12	SOFC 60%, SC 40%	2720	7.4	2755	7.5

The following sections show different combinations for a new energy system system and a mass statement for the different options.

4.1 Case 1: Lithium-ion batteries replaced by PEMFC

In the first scenario all the Lithium-ion batteries are replaced by PEM fuel cells. In table 17 the needed power from the solar cells is shown. In January and December 800 and 850 kW cannot be supplied (red marked). That is the worst case where just 70% of the electrical power could be delivered from solar cells. With having the maximum amount of solar cells installed the power for the engine sizes 5 and 6 cannot be supplied anyway in January and December. This means that the aircraft cannot raise up to 30 km altitude. But the normal flight range of 15 – 20 km could be reached without problems. The orange marked cells can be supplied but it excesses the maximum original value from the original model of 2.2 MW from table 10 in chapter 3.3 (in December, 850 kW thrust). Which means that the total possible amount of solar cells need to be installed and in worst case the power supplied for the engine will not exceed 750 kW in January or December. This orange marked cells shall just show the differences to the original model.
In table 17 also the quantity, the volume and the weight is mentioned. The volume is pretty small so there occurs no storage problem in the fuselage. Also the amount of batteries decreases drastically, thus also the battery weight decreases (see table 10).
It could be considered to design the solar system that it supplies $P_{70,Feb} = 2.1\ MW$ (total: $\frac{2.1\ MW}{0.7} = 3\ MW$) and so provides a flight height up to 30 km from February to November and in January and December the flight height is determined to the normal flight height at 20 km when the conditions are bad. Therefore, 19 panels along chord and 138 panels along span, 1,794 panels each wing, are needed with a weight of 47.2 kg. The fuel cell weight and amount equals the maximum value.

Table 17: PEM fuel cell, solar demand

Engine size	1	2	3	4	5	6
Month	**600 kW**	**650 kW**	**700 kW**	**750 kW**	**800 kW**	**850 kW**
	[W] $10^6 \cdot$					
JAN	1.89	2.04	2.2	2.36	2.51	2.67
FEB	1.42	1.53	1.67	1.79	1.90	2.02
MAR	1.2	1.3	1.4	1.5	1.6	1.7
APR	0.86	0.93	1.0	1.07	1.14	1.21
MAY	0.61	0.66	0.71	0.77	0.82	0.87
JUN	0.51	0.56	0.6	0.64	0.69	0.73
JUL	0.43	0.46	0.5	0.54	0.57	0.61
AUG	0.56	0.61	0.66	0.7	0.75	0.79
SEPT	0.73	0.79	0.85	0.91	0.97	1.03
OCT	1.01	1.1	1.18	1.27	1.35	1.44
NOV	1.43	1.55	1.67	1.79	1.9	2.02
DEC	1.89	2.04	2.2	2.36	2.51	2.67
PEMFC quantity	116	126	136	145	155	164
Volume (PEM) $[m^3]$	0.26	0.28	0.3	0.32	0.34	0.36
Weight (PEM) $[kg]$	212.4	226.4	240.4	253	267	279.6

4.2 Case 2: Lithium-ion batteries replaced by SOFC

In this scenario the Lithium-ion batteries are replaced by SOFC. In table 18 the power demanded by the fuel cells is shown for the different engine sizes and time of the year. The power shown in the red marked cells cannot be supplied by the solar cell system under bad conditions. So in worst cases the power for the engine sizes 4 to 6 cannot be fully delivered. So a raise up to 30 km altitude would be near to impossible. This problem can just occur in January or December. The orange marked cells can be supplied, they just exceed the maximum original value. Even when the maximum amount of solar cells is installed, problems occur in wintertime. From February to November the power for engine nr. 6 can be supplied without problems and also a raise in altitude is possible.
In the table also the quantity, the volume and the weight of the SOFC is mentioned. The volume is small so there will be no storage problems in the fuselage. Also the amount of batteries decreases drastically, even smaller than the PEMFC amount needed (see table 17), thus also the battery weight decreases but not as much as the weight decreases by using PEMFC. That is because the weight for one stack of SOFC is very high compared to PEMFC or Lithium-ion battery stack (also see table 10).
Here it could be considered that the solar system shall be designed to supply $P_{70,Feb} = 2.2\ MW$, (total: $\frac{2.2\ MW}{0.7} = 3.1\ MW$) which leads to the point that from February to November the aircraft could fly at altitudes up to 30 km if needed, and in January and December stays at 20 km altitude. Therefore, 2,698 panels are necessary on each wing with a weight of 48.6 kg and maximum installed quantity and hence weight for the SOFC.

Table 18: Solid oxid fuel cell, solar demand

Engine size	1	2	3	4	5	6
Month	**600 kW**	**650 kW**	**700 kW**	**750 kW**	**800 kW**	**850 kW**
	[W] $10^6 \cdot$					
JAN	2.03	2.2	2.37	2.54	2.71	2.88
FEB	1.54	1.67	1.79	1.92	2.05	2.18
MAR	1.29	1.4	1.51	1.62	1.72	1.83
APR	0.92	1.0	1.08	1.15	1.23	1.31
MAY	0.66	0.71	0.77	0.82	0.88	0.93
JUN	0.55	0.6	0.65	0.69	0.74	0.78
JUL	0.46	0.5	0.54	0.58	0.61	0.65
AUG	0.6	0.66	0.71	0.76	0.81	0.86
SEPT	0.78	0.85	0.91	0.98	1.04	1.11
OCT	1.09	1.18	1.27	1.36	1.45	1.55
NOV	1.54	1.67	1.79	1.92	2.05	2.18
DEC	2.03	2.2	2.37	2.54	2.71	2.88
SOFC quantity	65	70	75	81	86	91
Volume (SOFC) $[m^3]$	0.27	0.29	0.32	0.34	0.36	0.38
Weight (SOFC) $[kg]$	390	420	450	486	516	546

4.3 Case 3: Lithium-ion batteries and super capacitors

In this case the Lithium-ion batteries are replaced by a combination of Lithium-ion batteries and super capacitors. In tables 19 to 21 the respective powers needed from the installed solar cell system is shown.
In table 19 the energy storage system consists of 80% Lithium-ion batteries and 20% of super capacitors. The power needed from the solar cells is $P_{70,Jan} = 2.15\ MW$ (total $\frac{2.15\ MW}{0.7} = 3.07\ MW$) in January for engine size 6. Here the problem that not enough energy can be delivered in worst case during winter time does not exist. Therefore, 19 panels along chord and 141 panels along span, total 2,679 panels on each wing, are needed with a weight of 48.2 kg. The volume of the Lithium-ion batteries can be lowered about 2 – 3 m^3 due to the partial replacement with super capacitors. Also the weight can be reduced (around 150 kg weight loss) compared to the original system (see table 10).
In table 20 the energy storage system consists of 70% Lithium-ion batteries and 30% of super capacitors. The power needed from the solar cells is $P_{70,Jan} = 2.13\ MW$ (total $\frac{2.13\ MW}{0.7} = 3.04\ MW$). Therefore, 19 panels along chord and 139 panels along span, total 2,641 panels on each wing, are needed with a weight of 47.5 kg. Also the weight of Lithium batteries and thus the total battery weight decreases and the volume of the Lithium-ion battery stacks decreases compared to the scenario Lithium 80%/SC 20%.
In table 21 the system consists of 60% Lithium-ion batteries and 40% of super capacitors. The power needed from the solar cells is $P_{70,Jan} = 2.11\ MW$ (total $\frac{2.11\ MW}{0.7} = 3.01\ MW$). Therefore, 19 panels along chord and 138 panels along span, total 2,622 panels on each wing, are needed with a weight of 47.2 kg. Also the weight of needed Lithium-ion batteries and thus the total battery weight decreases and the volume of the Lithium-ion battery stacks decreases compared to the scenarios Lithium 80%/SC 20% and Lithium 70%/SC 30%.
In these three examples it is always possible to supply the 850 kW needed for the biggest engine and weight savings can be made by reducing the number

of solar panels. A raise in height shall be possible during the whole year even at bad conditions.

Table 19: Li 80%/Super capacitor 20%, solar demand

Engine size	1	2	3	4	5	6
Month	**600 kW**	**650 kW**	**700 kW**	**750 kW**	**800 kW**	**850 kW**
	[W] $10^6 \cdot$					
JAN	1.52	1.65	1.77	1.9	2.03	2.15
FEB	1.15	1.25	1.34	1.44	1.54	1.63
MAR	0.97	1.05	1.13	1.21	1.29	1.37
APR	0.69	0.75	0.81	0.86	0.92	0.98
MAY	0.49	0.53	0.58	0.62	0.66	0.69
JUN	0.41	0.45	0.48	0.52	0.55	0.59
JUL	0.35	0.37	0.40	0.43	0.46	0.49
AUG	0.45	0.49	0.53	0.57	0.60	0.64
SEPT	0.58	0.63	0.68	0.73	0.78	0.83
OCT	0.82	0.88	0.95	1.02	1.09	1.16
NOV	1.15	1.25	1.34	1.44	1.54	1.63
DEC	1.52	1.65	1.77	1.9	2.03	2.15
Super capacitor quantity	9	10	11	11	12	13
Battery quantity	393	425	458	491	523	556
Volume (Li-batteries)[m^3]	1.43	1.55	1.67	1.79	1.91	2.03
Weight (Li-batteries) [kg]	373.4	403.8	435.1	466.5	496.9	528.2
Weight (Super capacitor) [kg]	3.15	3.5	3.85	3.85	4.2	4.55

Table 20: Li 70% /Super capacitor 30%, solar demand

Engine size	1	2	3	4	5	6
Month	**600 kW**	**650 kW**	**700 kW**	**750 kW**	**800 kW**	**850 kW**
	[W] $10^6 \cdot$					
JAN	1.5	1.63	1.75	1.88	2.01	2.13
FEB	1.13	1.23	1.33	1.42	1.52	1.61
MAR	0.96	1.04	1.12	1.19	1.28	1.36
APR	0.68	0.74	0.79	0.85	0.91	0.97
MAY	0.49	0.53	0.57	0.61	0.65	0.69
JUN	0.41	0.44	0.48	0.51	0.55	0.58
JUL	0.34	0.37	0.39	0.43	0.46	0.48
AUG	0.45	0.49	0.52	0.55	0.59	0.63
SEPT	0.58	0.63	0.67	0.72	0.77	0.82
OCT	0.81	0.88	0.94	1.01	1.08	1.14
NOV	1.14	1.23	1.33	1.42	1.52	1.61
DEC	1.5	1.63	1.75	1.88	2.01	2.13
Super capacitor quantity	14	15	16	17	18	19
Battery quantity	344	372	401	429	458	487
Volume (Li-batteries)[m^3]	1.25	1.36	1.46	1.56	1.67	1.77
Weight (Li-batteries)[kg]	326.8	353.4	380.9	407.6	435.1	462.7
Weight (Super capacitors)[kg]	4.9	5.3	5.6	6	6.3	6.7

Table 21: Li 60%/Super capacitor 40%, solar demand

Engine size	1	2	3	4	5	6
Month	**600 kW**	**650 kW**	**700 kW**	**750 kW**	**800 kW**	**850 kW**
	[W] $10^6 \cdot$					
JAN	1.49	1.61	1.74	1.86	1.98	2.11
FEB	1.13	1.22	1.31	1.41	1.5	1.59
MAR	0.95	1.03	1.1	1.18	1.26	1.34
APR	0.68	0.73	0.79	0.85	0.90	0.96
MAY	0.48	0.52	0.56	0.6	0.64	0.68
JUN	0.41	0.44	0.47	0.51	0.54	0.57
JUL	0.34	0.37	0.39	0.42	0.45	0.48
AUG	0.44	0.48	0.52	0.55	0.59	0.63
SEPT	0.57	0.62	0.67	0.72	0.76	0.81
OCT	0.79	0.87	0.93	0.99	1.07	1.13
NOV	1.13	1.22	1.31	1.41	1.5	1.59
DEC	1.49	1.61	1.74	1.86	1.98	2.11
Super capacitor quantity	18	19	21	22	24	25
Battery quantity	295	319	344	368	393	417
Volume (Li-batteries)[m^3]	1.07	1.16	1.25	1.34	1.43	1.52
Weight (Li-batteries)[kg]	280.3	303.1	326.8	349.6	373.4	396.2
Weight (Super capacitors)[kg]	6.3	6.7	7.4	7.7	8.4	8.8

4.4 Case 4: PEMFC and super capacitors

Here the PEM fuel cells from paragraph 4.1 are replaced by a combination of PEMFC and super capacitors. In tables 22 to 24 three different combinations are shown and the respective power the solar system need to supply.
In table 22 the energy storage system comprise of 80% PEM fuel cells and 20% of super capacitors. Here, the red marked cells exceed the maximum amount of solar power which can be supplied for worst conditions (P_{70}). So a raise up to 30 km is not possible under bad conditions in January and December. From February to November the power for engine nr. 6 can be supplied and also a raise in altitude is possible. The orange marked cells can be supplied but they just show that they exceed the maximum value of the original model (see table 10).
The solar cell system could be designed to deliver $P_{70,Feb} = 2\ MW$ (total: $\frac{2\ MW}{0.7} = 2.9\ MW$) so that in January and December the aircraft shall stay at 20 km altitude and during February and November it can even climb up to 30 km. Therefore, 18 panels along the chord and 140 along the span, total 2,520 panels on each wing, are needed with a weight of 45.4 kg. Since the mass of the PEMFC stack was already lower than the mass of SOFC stack the mass still decreases by also using partly super capacitors.
In table 23 the energy storage system consists of 70% PEM fuel cells and 30% of super capacitors. The red marked cells exceed the maximum amount of solar power which can be supplied for worst conditions. So a raise up to 30 km is not possible in January and December. But the value is just a little bit over the top value of $P_{el,70}$ from chapter 3.2: $P_{el,70} = 2.42\ MW$, and here $P_{70} = 2.46\ MW$. From February to November the power for engine nr. 6 can be supplied and also a raise in altitude is possible. The orange marked cells just show that they exceed the original model's maximum value.
The solar cell system is designed to deliver $P_{70,Feb} = 1.9\ MW$ (total: $\frac{1.9\ MW}{0.7} = 2.7\ MW$) so that in January and December the aircraft shall stay at 20 km altitude at bad conditions and during February and November it can even climb up to 30 km. Therefore, 17 panels along chord and 138 along the span, total 2,346 panels each wing, are needed with a weight of

42.2 kg. Mass and volume of the PEMFC decreases, so the total fuel cell system weight and hence the total aircraft weight decreases.
In table 24 the energy storage system consists of 60% PEM fuel cells and 40% of super capacitors. The orange marked cells just show that they exceed the original maximum value. So during the whole year the power of 850 kW for the engine can be supplied even at worse conditions (here: $P = 2.39\ MW$, see table 24 and from original model $P_{el,70} = 2.42\ MW$, see table 10).
The solar cell system shall be redesigned anyway since it is fine when during worse conditions the aircraft cannot raise up to 30 km (in January or December). It is designed to deliver $P_{70,Feb} = 1.9\ MW$ (total: $\frac{1.9\ MW}{0.7} = 2.7\ MW$) like the scenario PEMFC 70%/ SC 30%. So 2,346 panels shall be on each wing with a weight of 42.2 kg. The weight and the volume is smaller than in the scenario PEMFC 70%/ SC 30% because more super capacitors replace more PEMFC and the super capacitors are lighter.
The solar cell system was designed to deliver most time of the year the power amount needed to climb up to 30 km altitude if needed. Since this could lead to problems under worse conditions in January and December, the reference point was set to the needed power for the engine size 6 in February.

Table 22: PEM 80% /Super capacitor 20%, solar demand

Engine size	1	2	3	4	5	6
Month	**600 kW**	**650 kW**	**700 kW**	**750 kW**	**800 kW**	**850 kW**
	[W] $10^6 \cdot$					
JAN	1.79	1.94	2.08	2.23	2.38	2.53
FEB	1.35	1.47	1.58	1.69	1.8	1.92
MAR	1.14	1.23	1.33	1.42	1.52	1.61
APR	0.81	0.88	0.95	1.02	1.08	1.15
MAY	0.58	0.63	0.68	0.73	0.77	0.82
JUN	0.49	0.53	0.57	0.61	0.65	0.69
JUL	0.41	0.44	0.47	0.51	0.54	0.58
AUG	0.53	0.58	0.62	0.67	0.71	0.75
SEPT	0.69	0.74	0.80	0.86	0.92	0.97
OCT	0.96	1.04	1.12	1.19	1.28	1.36
NOV	1.35	1.47	1.58	1.69	1.8	1.92
DEC	1.79	1.94	2.08	2.23	2.38	2.53
Super capacitor quantity	9	10	11	11	12	13
PEMFC quantity	93	101	109	116	124	132
Volume (PEM)[m^3]	0.21	0.22	0.24	0.26	0.27	0.29
Weight (PEM)[kg]	130.2	141.4	152.6	162.4	173.6	184.8
Weight (Super capacitor) [kg]	3.15	3.5	3.85	3.85	4.2	4.55

Table 23: PEM 70% /Super capacitor 30%, solar demand

Engine size	1	2	3	4	5	6
Month	**600 kW**	**650 kW**	**700 kW**	**750 kW**	**800 kW**	**850 kW**
	[W] 10^6·					
JAN	1.74	1.88	2.03	2.17	2.32	2.46
FEB	1.32	1.43	1.54	1.64	1.75	1.86
MAR	1.11	1.19	1.29	1.38	1.47	1.57
APR	0.79	0.86	0.92	0.99	1.05	1.12
MAY	0.56	0.61	0.66	0.7	0.75	0.79
JUN	0.47	0.51	0.55	0.59	0.63	0.67
JUL	0.39	0.43	0.46	0.49	0.53	0.56
AUG	0.52	0.56	0.6	0.65	0.69	0.73
SEPT	0.67	0.72	0.78	0.84	0.89	0.95
OCT	0.93	1.01	1.09	1.17	1.24	1.32
NOV	1.32	1.43	1.54	1.64	1.75	1.86
DEC	1.74	1.88	2.03	2.17	2.32	2.46
Super capacitor quantity	14	15	16	17	18	19
PEMFC quantity	82	88	95	102	109	115
Volume (PEM)[m^3]	0.18	0.19	0.21	0.23	0.24	0.25
Weight (PEM)[kg]	114.8	123.2	133	142.8	152.6	161
Weight (Super capacitors)[kg]	4.9	5.3	5.6	6	6.3	6.7

Table 24: PEM 60% /Super capacitor 40%, solar demand

Engine size	1	2	3	4	5	6
Month	**600 kW**	**650 kW**	**700 kW**	**750 kW**	**800 kW**	**850 kW**
	[W] 10^6·					
JAN	1.69	1.83	1.97	2.11	2.25	2.39
FEB	1.28	1.38	1.49	1.59	1.7	1.81
MAR	1.07	1.16	1.25	1.34	1.43	1.52
APR	0.77	0.83	0.89	0.96	1.02	1.09
MAY	0.55	0.59	0.64	0.68	0.73	0.78
JUN	0.46	0.49	0.54	0.58	0.61	0.65
JUL	0.38	0.42	0.45	0.48	0.51	0.54
AUG	0.5	0.54	0.59	0.63	0.67	0.71
SEPT	0.65	0.7	0.76	0.81	0.87	0.92
OCT	0.91	0.98	1.06	1.13	1.21	1.28
NOV	1.28	1.38	1.49	1.59	1.7	1.81
DEC	1.69	1.83	1.97	2.11	2.25	2.39
Super capacitor quantity	18	19	21	22	24	25
PEMFC quantity	70	76	82	87	93	99
Volume (PEM)[m^3]	0.15	0.17	0.18	0.19	0.21	0.22
Weight (PEM)[kg]	98	106.4	114.8	121.8	130.2	138.6
Weight (Super capacitors)[kg]	6.3	6.7	7.4	7.7	8.4	8.8

4.5 Case 5: SOFC and super capacitors

In this case SOFC from paragraph 4.2 are replaced by a combination of SOFC and super capacitors. In tables 25 to 27 three different combinations are shown and its respective power the solar system need to deliver.
In table 25 the energy storage system consists of 80% SOFC and 20% of super capacitors. The red marked cells exceed the maximum amount of power which can be delivered from the solar cell system. So a raise up to 30 km is not possible in January and December. From February to November the power can be supplied. The orange marked cells can be supplied but they just show that they exceed the original model's maximum value.
In solar cell system is designed to deliver $P_{70,Feb} = 2.1\ MW$ (total: $\frac{2.1\ MW}{0.7} = 3\ MW$). Therefore, 19 panels along chord and 138 panels along span, total 2,622, are needed. The weight of these cells is 47.2 kg. The weight of the storage system is lower than from the original model but still high. That is because of the SOFC has already a high weight per stack. In table 26 the battery system comprises of 70% SOFC and 30% of super capacitors. Here, the red marked cells exceed the maximum amount of solar power which can be supplied for worst conditions in January and December. So a raise up to 30 km is then not possible. During the rest of the year the power can also be supplied for engine sizes 5 and 6 and also a raise in altitude is possible. The orange marked cells can be supplied but they show that they exceed the original's maximum value.
The solar cell system is designed to deliver $P_{70,Feb} = 2\ MW$ (total: $\frac{2\ MW}{0.7} = 2.9\ MW$). Therefore, 18 panels along the chord and 140 along the span, total 2,520 panels on each wing, are needed with a weight of 45.4 kg. Mass and volume of the SOFC decreases when more SOFC are replaced with super capacitors and also the total fuel cell system's weight decreases.
In table 27 the energy storage system comprises of 60% SOFC and 40% of super capacitors. Here, the red marked cells exceed the maximum amount of solar power which can be supplied ($P_{el,70} = 2.42\ MW$ from chapter 3.2) so in January and December a climbing up to 30 km is not possible at worse conditions. During the rest of the year the power can also be supplied for

engine size 6. The orange marked cells show that they exceed the original model's maximum value.
The solar cell system shall deliver $P_{70,Feb} = 2\ MW$ (total: $\frac{2\ MW}{0.7} = 2.9\ MW$) like in scenario SOFC 70%/SC 30%. Hence, 2,520 panels are installed on each wing with a weight of 45.4 kg. Mass and volume of the SOFC decreases like the whole system decreases in mass.
The solar cell system was designed to deliver most time of the year the power amount needed to climb up to 30 km altitude. Since this can be a problem under worse conditions in January and December, the reference point is then the needed power for the engine size 6 in February. Not exactly the needed amount from February is taken, but very close (a bit overestimated), since it was not possible to reach exactly the needed power amount with the solar cells. But the given estimation is pretty close to the real value from February.

Table 25: SOFC 80% /Super capacitor 20%, solar demand

Engine size	1	2	3	4	5	6
Month	**600 kW**	**650 kW**	**700 kW**	**750 kW**	**800 kW**	**850 kW**
	[W] 10^6.					
JAN	1.9	2.06	2.22	2.38	2.54	2.69
FEB	1.44	1.56	1.68	1.8	1.92	2.04
MAR	1.21	1.31	1.41	1.51	1.61	1.72
APR	0.86	0.94	1.01	1.08	1.15	1.23
MAY	0.62	0.67	0.72	0.77	0.82	0.88
JUN	0.52	0.56	0.61	0.65	0.69	0.74
JUL	0.43	0.47	0.5	0.54	0.58	0.61
AUG	0.57	0.61	0.66	0.71	0.76	0.8
SEPT	0.73	0.79	0.85	0.91	0.98	1.04
OCT	1.02	1.11	1.19	1.28	1.36	1.45
NOV	1.44	1.56	1.68	1.8	1.92	2.04
DEC	1.9	2.06	2.22	2.38	2.54	2.69
Super capacitor quantity	9	10	11	11	12	13
SOFC quantity	52	56	60	65	69	73
Volume (SOFC)[m^3]	0.19	0.2	0.22	0.24	0.25	0.27
Weight (SOFC)[kg]	260	280	300	325	345	365
Weight (Super capacitor) [kg]	3.15	3.5	3.85	3.85	4.2	4.55

Table 26: SOFC 70% /Super capacitor 30%, solar demand

Engine size	1	2	3	4	5	6
Month	**600 kW**	**650 kW**	**700 kW**	**750 kW**	**800 kW**	**850 kW**
	[W] 10^6.					
JAN	1.84	1.99	2.14	2.29	2.45	2.6
FEB	1.39	1.51	1.62	1.74	1.86	1.97
MAR	1.17	1.27	1.36	1.46	1.56	1.66
APR	0.84	0.91	0.97	1.04	1.11	1.18
MAY	0.59	0.65	0.69	0.75	0.79	0.85
JUN	0.5	0.54	0.58	0.63	0.67	0.71
JUL	0.42	0.45	0.49	0.52	0.56	0.59
AUG	0.55	0.59	0.64	0.68	0.73	0.78
SEPT	0.71	0.77	0.82	0.88	0.94	1.0
OCT	0.99	1.07	1.15	1.23	1.32	1.39
NOV	1.39	1.51	1.62	1.74	1.85	1.97
DEC	1.84	1.99	2.14	2.29	2.45	2.6
Super capacitor quantity	14	15	16	17	18	19
SOFC quantity	45	49	53	57	60	64
Volume (SOFC)[m^3]	0.16	0.18	0.19	0.21	0.22	0.23
Weight (SOFC)[kg]	225	245	265	285	300	320
Weight (Super capacitors)[kg]	4.9	5.3	5.6	6	6.3	6.7

Table 27: SOFC 60% Super capacitor 40%, solar demand

Engine size	1	2	3	4	5	6
Month	**600 kW**	**650 kW**	**700 kW**	**750 kW**	**800 kW**	**850 kW**
	[W] 10^6·					
JAN	1.77	1.92	2.07	2.22	2.37	2.51
FEB	1.34	1.46	1.57	1.68	1.79	1.9
MAR	1.13	1.22	1.32	1.41	1.51	1.59
APR	0.81	0.87	0.94	1.01	1.08	1.14
MAY	0.58	0.62	0.67	0.72	0.77	0.82
JUN	0.48	0.52	0.56	0.60	0.65	0.69
JUL	0.4	0.44	0.47	0.5	0.54	0.57
AUG	0.53	0.57	0.62	0.66	0.7	0.75
SEPT	0.68	0.74	0.79	0.85	0.91	0.97
OCT	0.95	1.03	1.11	1.19	1.27	1.35
NOV	1.34	1.46	1.57	1.68	1.79	1.9
DEC	1.77	1.92	2.07	2.22	2.36	2.51
Super capacitor quantity	18	19	21	22	24	25
SOFC quantity	39	42	45	49	52	55
Volume (SOFC)[m^3]	0.14	0.15	0.16	0.18	0.19	0.2
Weight (SOFC)[kg]	195	210	225	245	260	275
Weight (Super capacitors)[kg]	6.3	6.7	7.4	7.7	8.4	8.8

4.6 Weight

In table 28 the maximum weights for the 6 engine sizes are shown. Engine size 1 represents the needed power to stay at 20 km height and the engine size 6 stays for the climbing up to maximum 30 km height. In all cases the battery amount and type and hence the weight of the energy storage system changes. Of course the amount of solar cells which need to be installed is changing. Favorable is that the solar panels deliver enough power for the 850 kW engine. So for the scenarios where the Lithium-ion batteries were replaced by PEM or SOFC the maximum amount of solar cells is needed to supply this the power of the engine. Also for the cases PEM 80%/ SC 20%, PEM 70%/ SC 30%, PEM 60%/ SC 40%, SOFC 80%/ SC 20%, SOFC 70%/ SC 30% and SOFC 60%/ SC 40% the total amount of solar cells are needed. But even with the total amount of solar cells installed in this cases it is not save that the needed energy could be supplied for worst conditions, which means shadowing and the effect of declination in January and December (red marked cells from the tables before). For the scenarios including Lithium-ion batteries (original model, LI 80%/ SC 20%, LI 70%/ SC 30%, LI 60%/ SC 40%) and the maximum amount of solar cells is not necessary for supplying the needed power for an engine size 6. The total weight of solar cells just contribute 54 kg to the whole weight but is not considered in the table because this shall just show an overview. Also the weight loss for engine size 6 would be for the original model 5.4 kg, for LI 80%/ SC 20% 5.8 kg, for LI 70%/ SC 30% 6.5 kg and for the case LI 60%/ SC 40% the weight loss is 6.8 kg. The red marked row in table 28 shows the values of the original system and this is also the heaviest. Even when subtracting the weight from the not needed solar panels from the Lithium-ion battery combinations models, nothing changes in the hierarchy: the second heaviest aircraft model would be with SOFC as energy storage system, followed by all the Lithium-ion combinations LI 80%/ SC 20%, LI 70%/ SC 30% and LI 60%/ SC 40%. A bit lighter are the models with the SOFC/ SC energy storage system, followed by the PEM model, the PEM 80 %/ SC 20 % and the PEM 70%/ SC 30% models. The blue marked row in the table shows the scenario PEMFC 60% /SC 40%. This

is the lightest model with 377 kg maximum weight of the HALE aircraft. The total installable amount of solar panels, hence the maximum mass for solar panels is added to each of the models without considering the possible weight losses. Since engine size 6 is favorable and not every model can deliver the needed power during the whole year the total amount of solar cells is here added and maybe the needed amount of power could be delivered when there are not the worst conditions in wintertime. The better solutions in this case, where the needed power cannot be delivered in wintertime, are mentioned in each model's paragraph. There engine size 6 and February were the reference points. These solutions are mentioned again in chapter 5.
The super capacitors which are placed on the underpart of the wings do not exceed the tensile and bending strengths. Also the maximum installable amount of super capacitors is never exceeded.

Table 28: Mass statement, maximum solar panels installed *

Engine size	1	2	3	4	5	6
	600 kW	**650 kW**	**700 kW**	**750 kW**	**800 kW**	**850 kW**
Original	696	735	773	812	851	890
PEM	392	406	420	433	447	459
SOFC	605	630	655	685	710	735
PEM 80 %, SC 20 %	363	374	386	396	407	419
PEM 70 %, SC 30 %	349	358	368	378	388	397
PEM 60 %, SC 40 %	334	343	352	359	368	377
LI 80 %, SC 20 %	606	637	669	700	730	762
LI 70 %, SC 30 %	561	588	616	643	671	699
LI 60 %, SC 40 %	516	539	564	587	611	634
SOFC 80 %, SC 20 %	493	513	533	558	579	599
SOFC 70 %, SC 30 %	459	480	500	521	536	556
SOFC 60 %, SC 40 %	431	446	462	482	498	513

* Here the total masses for the different energy storage models for the different engine sizes are shown. The total installable amount of solar panels, hence the maximum mass for solar panels is added to each of the models without considering the possible weight losses. But since engine size 6 is favorable and not every model can deliver the needed power during the whole year the total amount of solar cells is here considered for each energy storage model and each engine size.

Chapter 5

Results, Discussion and Summary

In this chapter a valid solar cell system is set for each model, like the ones already mentioned in chapter 4, and an explanation why the solar cell system is chosen to supply this amount as well as the resulting benefits and obstacles are explained. The energy storage system equals the maximum calculated energy storage system weight and the engine size 6 which needs 850 kW (2 kV, $\eta_{Propulsion} = 0.82$) is the chosen engine for the aircraft. The adapted amount of solar cells and the corresponding weight are listed in tables 29 and 30.

The lightest values for energy storage system and solar cells system are reached with the PEMFC 60%/ SC 40% model, followed by the other PEMFC combinations and then the PEMFC model where just PEM fuel cells are used to function as energy storage system. After that the SOFC 60%/ SC 40% model, followed by the SOFC 70%/ SC 30% model and the SOFC 80%/ SC 20% model are following. Thereafter, the LI 60%/ SC 40% model, the LI 70%/ SC 30% model, the SOFC model and subsequently the LI 80%/ SC 20% model are coming. The original model is the heaviest model. So with each of the other models an improvement in total weight of the aircraft could be made by lowering the weights of the energy storage system and the installed panels.

The next step is to determine the real total mass of each model. Therefore the assumed weights for communication and heating systems as well as some additional weight stay the same for each model, even when the SOFC models shall have the highest weight from these because of the improved heating system and surplus of insulation needed. Unfortunately, this could not be determined sufficiently, so for all models the same values are taken into account. The power needed and hence the installed solar panels change for each model. This is listed in table 29. In this table also the amount of installed solar panels per wing, the total solar power output and the possibility of climbing up to 30 km all year around is shown. If the aircraft can climb up to 30 km all year around is not a very important factor. The climbing is also just limited under worst conditions in January and December. Every model can fly at 20 km altitude and that is a requirement of HALE aircrafts. The installed panels and respectively their power output is the lowest for the PEM 60%/ SC 40% model.

Table 29: Results, engine 850 kW *

	Model	**Total aircrafts's weight [kg]**	**Installed panels, one wing**	**Total power output solar [MW]**	**Possibility of climbing up to 30 km all year**
0	MAX. Original	890	3,000	3.5	YES
1	Original	884.6	2,698	3.1	YES
2	PEM	452.4	2,622	3.0	NO
3	SOFC	729.2	2,698	3.1	NO
4	LI 80 %, SC 20 %	756.5	2,679	3.07	YES
5	LI 70 %, SC 30 %	692.4	2,641	3.04	YES
6	LI 60 %, SC 40 %	627.7	2,622	3.01	YES
7	PEM 80 %, SC 20 %	410.3	2,520	2.9	NO
8	PEM 70 %, SC 30 %	385.4	2,346	2.7	NO
9	PEM 60 %, SC 40 %	365.1	2,346	2.7	YES
10	SOFC 80 %, SC 20 %	592.3	2,622	3	NO
11	SOFC 70 %, SC 30 %	547.6	2,520	2.9	NO
12	SOFC 60 %, SC 40 %	504.7	2,520	2.9	NO

* In this table the aircraft's weight, installed solar panels on each wing and their total power output as well as the possibility of climbing up to 30 km all year around for each model are shown.

The masses of the energy storage system and the corresponding installed solar cell system are shown in table 30. Here you can see that the differences in weight of the energy storage system and of the solar cell system are enormous. While the solar cell system contributes almost nothing to the total mass of the aircraft, the energy storage system contributes around 40 – 70% to the total weight of the aircraft.

Table 30: Masses energy storage and solar system, engine 850 kW *

	Model	**Energy storage system [kg]**	**Solar cell system [kg]**
1	Original	660	48.6
2	PEM	229.6	47.2
3	SOFC	505	48.2
4	LI 80 %, SC 20 %	532.8	47.5
5	LI 70 %, SC 30 %	469.3	47.5
6	LI 60 %, SC 40 %	404.9	47.2
7	PEM 80 %, SC 20 %	189.4	45.4
8	PEM 70 %, SC 30 %	167.7	42.2
9	PEM 60 %, SC 40 %	147.4	42.2
10	SOFC 80 %, SC 20 %	369.6	47.2
11	SOFC 70 %, SC 30 %	326.7	45.4
12	SOFC 60 %, SC 40 %	283.8	45.4

* In this table the masses for the energy storage system and for the solar cell system for the different models are shown. Here the masses are just shown for the engine size 6 (850 kW).

In the beginning of the thesis was stated that the battery weight contribute a lot to the total weight of the aircraft. Therefore, the contribution of the energy storage systems to the total weight in percent is shown in table 31. Here you see that for almost every model the storage system contributes over 50% to the total mass, except the PEM/ SC combinations. From the original model the batteries contribute almost 75% to the total weight. So there is still a lot of space for improvement since a lighter aircraft is more favorable.

Table 31: Contribution battery system to total mass *

	Model	**Storage system [kg]**	**Total mass [kg]**	**Percentage [%]**
0	Original	660	884.6	74.6
2	PEM	229.6	452.4	50.8
3	SOFC	505	729.2	69
4	LI 80 %, SC 20 %	532.8	756.5	70
5	LI 70 %, SC 30 %	469.3	692.4	68
6	LI 60 %, SC 40 %	404.9	627.7	65
7	PEM 80 %, SC 20 %	189.4	410.3	46
8	PEM 70 %, SC 30 %	167.7	385.4	44
9	PEM 60 %, SC 40 %	147.4	365.1	40
10	SOFC 80 %, SC 20 %	369.6	592.3	62
11	SOFC 70 %, SC 30 %	326.7	547.6	60
12	SOFC 60 %, SC 40 %	283.8	504.7	56

* In this table the masses for the energy storage system in comparison to the total mass of the aircraft for the different models are shown. Here the masses are just shown for the engine size 6 (850 kW). Also the percentage the energy storage system contributes to the total mass of each model is given.

Next the benefits and obstacles of the different systems are mentioned.
The original model with Lithium-ion batteries is mostly used nowadays because the Lithium-ion batteries are good known and lot of their obstacles are eliminated, other ways skipped or already improved. Still great obstacles are the high weight and the low lifetime of these batteries so there is still enough room for improvement or the battery system is just completely or partly replaced by other energy storage systems like fuel cells and /or super capacitors. Due to experience, there occur lots of malfunctions and failures during longer operation. For the original model where just the Lithium-ion batteries are used the real lifetime would be around $1 - 2$ years (2 years in best case) and not much longer in best cases, even though the lifetime would be quite high in theory.
PEM fuel cells, also known as light weight fuel cells, happen to be the lightest models from all models mentioned in this paper. Also the PEMFC is highly developed and is cheap compared to the other possible options. On the other side these fuel cells react very sensitive on changings in closed environment and they need pure hydrogen to provide best output and least maintenance or malfunctions. So they have to be regulated very strictly. Also, due to experience, there occur lots of malfunctions and failures during longer operation. For the model where just PEMFC are used the real lifetime would be around 8 months and not much longer in best cases, even though the lifetime would be quite high in theory.
Solid oxide fuel cells are on the one hand heavy and operating at very high temperatures. So a better heating system and better insulation is needed than when using Lithium-ion batteries or PEMFC as energy storage system. On the other hand these fuel cells are not as demanding as PEMFC regarding the fuel. They do not need pure Hydrogen just a Hydro-compound like Hydrocarbon is fine. Even when they are quite heavy compared to the others, the power output of one stack is higher and thus compensates this. Moreover, when looking at the weight balances the SOFC (combinations) they are not the heaviest ones. The Lithium-ion combinations are still heavier than the SOFC models. Due to experience, there occur often failures during longer operation. For the model where just SOFC are used the real

lifetime would be 7 – 12 months, even though the lifetime would be quite high in theory.
This lifetimes are gathered from experiments from mobile applications and not directly from experiences from HALE aircrafts. Since this is a quite new development there are not enough data collected yet but for the future lots of projects regarding HALE aircrafts are in progress. The longest flight of a HALE aircraft took 15 days so far. It was not just determined by the energy storage system, also the on-board equipment tends to fail. So it will take some time to gather also valid information from HALE aircraft flights.
So the lifetime in reality is dependent on various other factors then the theoretical lifetime. Here the Lithium-ion batteries have a slightly higher lifetime than SOFC and PEMFC which have similar lifetimes. All these real lifetimes are based on experiences and statistical values for tending to malfunction or failure.
Super capacitors are good when energy need to be delivered immediately and they are very good in this because of their high power density. Since the energy density is pretty low the super capacitors are not good when storing energy a longer time. That is why nowadays super capacitors are just used in combinations as energy storage. The energy can be stored longer in batteries and when there is an immediate demand the super capacitor could deliver and fast recharge again without the lifetime of the super capacitor suffers much. With this "split of labor" also the lifetime of the batteries respectively the fuel cells is increased. Here, it is hard to give concrete values for the lifetime, since it is an incipient development, but for the combinations where 30% or 40% are super capacitors improvements in lifetime up to 25% are experienced.
Generally, a system combination with super capacitors is favorable. Because of the super capacitors the energy storage system's weight and hence the total aircraft weight is lowered. Since the quantity of the batteries or fuel cells is reduced also the volume of the system which is installed in the fuselage is lowered and thus there is more free space available in the fuselage (e.g. for more equipment for more complex missions).
PEMFC combinations are better than when just the fuel cells act as storage

system. With super capacitors the lifetime and hence the flight endurance could be enlarged. The same goes for SOFC combinations and Lithium-ion combinations with super capacitors. Like mentioned before the real lifetime could be increased up to 25% with replacing some batteries or fuel cells with super capacitors.

Total amount of solar cells and the respective total solar power output are also shown in table 29. Again the PEM 60%/ SC 40% model demands the lowest amount from solar power and still has the possibility to climb up to 30 km during the whole year, even at worst conditions. This is also the recommendation as a replacement for the Lithium-ion battery storage system (original model). Also the other two PEM/ SC combinations would give a good solution even though when they could not climb higher than 20 km all year around. Since the stated points from the beginning of this paper, what a HALE aircraft shall fulfill (high altitude: 20 km, long endurance: minimum 24 h), are fulfilled, it would be a good replacement. Also all other models fulfill the requirements but the PEMFC/ SC combinations provide a lower demand of solar power and are lighter than the other proposed models.

Chapter 6

Conclusion

After determining the weights of each aircraft's part and the needed power for the different models, the recommendation is to use a combination of proton exchange membrane fuel cells and super capacitors as energy storage system. The energy storage system, which suits best, consists of 60 % of proton exchange membrane fuel cells and 40 % of super capacitors. Here the best results for lifetime of the energy storage system as well as the storage system's weight and the total weight of the aircraft are achieved.

HALE aircrafts powered by sustainable energy sources are a technology of the future. There are many alternative energy solutions that are promising; including bio-fuel and hydrogen fuel cells as only energy source, but nothing is as limitless as solar technology. But for nowadays technology the HALE aircraft has not a long enough endurance to send it on longer missions. It could fly until the energy storage system need to be replaced or repaired and, in theory, the battery system has a quite fine lifetime. But in reality due to not fully developed technologies and the conditions at these altitudes (e. g. very high and very low temperatures, cosmic rays) the energy storage system as well as all other systems and equipment (e.g. heating and communication) are vulnerable for preterm failures. The longest mission ever took two weeks but in order to ensure the technology and hence any project sustainability, also including cost-effective benefits, the flight duration must increase up to a

continuous flight for at least six months. This leads to a continuous research and improvement in solar cells and energy storage systems, because these are the most critical parts. So as time goes on and more and more projects regarding HALE aircrafts are running, the more can be improved with these new collected data.
HALE aircrafts are a very promising incipient technology but still a lot of space for improvement is given on this field.

Bibliography

[1] Armin G Aberle. Thin-film solar cells. *Thin Solid Films*, 517(17):4706–4710, 2009.

[2] National Aeronautics and Space Administration (NASA). Wing Geometry Definitions, last update June 2014.

[3] Guglielmo S. Aglietti, Stefano Redi, Adrian R. Tatnall, and Thomas Marvart. Harnessing High-Altitude Solar Power. *IEEE*, 2009.

[4] Rolf J. Ahlers and Sylvia Rohr. *Forum Luft- und Raumfahrt: Chancen und Potenziale für Luft- und Raumfahrt.* Steinbeis-Edition, 2005.

[5] Astris. Aufbau eines Satelliten, 2011.

[6] Manish R. Bhatt. Solar unmanned aerial vehicle: High altitude long endurance applications. Technical report, Department of Mechanical and Aerospace Engineering, 2012.

[7] Franz Bischof. Strömungsmechanik, EN/UT 2, Bachelor, 2014.

[8] WH Bloss, F Pfisterer, M Schubert, and T Walter. Thin-film solar cells. *Progress in Photovoltaics: Research and Applications*, 3(1):3–24, 1995.

[9] My blue planet. Sonnenenergie gibt's im Überfluss., last update 2014.

[10] Leopold Böswirth. *Technische Strömungslehre: Lehr- und Übungsbuch.* Vieweg+Teubner Verlag, 2007.

[11] F. Soavi C. Arizzani, M. Mastragostino. New trends on electrochemical supercapacitors. *Journal of Powers*, 2001.

[12] Enrico Cestino. Design of solar high altitude long endurance aircraft for multi payload and operations. *ScienceDirect, Aerospace Science and Technology*, 2006.

[13] Big Frog Mountain Corporation. PowerFilm, 2011.

[14] Andrea Davide. *Battery Management Systems for Large Lithium Ion Battery Packs*. Artech House Inc, 2010.

[15] F Dörrscheidt et al. 1 grundbegriffe der regelungstechnik. 1989.

[16] Dr. Günter Dietrich Dr. Peter Kurzweil. Bindeglied zwischen Kondensatoren und Batterien. *Dornier*, 2012.

[17] A. Y. Dvorkin and E. H. Steinberger. Modeling the altitude effect on solar UV radiation. *Solar Energy*, 1998.

[18] B. M. Eid, J. Chebil, F. Albatsh, and W. F. Faris. International Conference on Mechatronics. In *Challanges of Integrating Unmanned Aerial Vehicles In Civil Applications*, 2013.

[19] Wikipedia Encyclopedia. Thin-film solar cell, 2013.

[20] Farivar Fazelpour, Majid Vafaeipour, Omid Rahbari, and Reza Shirmohammadi. Considerable parameters of using PV cells for solar-powered aircrafts. *Renewable and Sustainable Energy Reviews*, 2013.

[21] Walter Flury. Zur bahnberechnung von geostationären satelliten. *Celestial mechanics*, 7(3):376–383, 1973.

[22] Elzbieta Frackowiak. Carbon materials for supercapacitor application. *Physical Chemistry Chemical Physics*, 9(15):1774–1785, 2007.

[23] Bernhard Frenzel. Strömungslehre: Aerodynamik, EN/UT 2, Bachelor, 2009.

[24] Bernhard Frenzel. Aerodynamik während des Fluges, 2010.

[25] Klaus Fuest and Peter Döring. *Elektrische Maschinen und Antriebe*. Vieweg+Teubner Verlag, 2007.

[26] Zdobyslaw Goraj, Andrzej Frydrychiewicz, and Jacek Winiecki. Design concept of a high-altitude long-endurance unmanned aerial vehicle. *Elsevier Science*, 1999.

[27] Jörg Haun. Brennstoffzelle in der Raumfahrt. Technical report, Fachhochschule Darmstadt, Deutschland, 2005.

[28] Thomas Hildebrand. Strömungsmechanik, MB 2, Bachelor, 2012.

[29] Mustapha Jammal. *Stand der Technik und Anwendung von Superkondensatoren*. Grin Verlag Gmbh, 2013.

[30] Philip J Jarrett. *Aircraft for Fun: Light and Privately-built Aircraft*. Putnam Aeronautical, 2011.

[31] Frank Kameier. Aerodynamische und akustische grundbegriffe.

[32] Achmed A. W. Khammas. Buch der Synergie, last update 2014.

[33] Reiner Korthauer. *Handbuch Lithium-Ionen-Batterien*. Springer Vieweg, 2013.

[34] Peter Kurzweil. Brennstoffzellen, EN/UT 4, Bachelor, 2012.

[35] Peter Kurzweil. *Brennstoffzellentechnik: Grundlagen, Komponenten, Systeme, Anwendungen*. Springer, 2012.

[36] Leonid Leiva. Memory effect now also found in lithium-ion batteries, 2013.

[37] Jae Hoon Lim, Sun Choi, Sang Joon Shin, and Dong-Ho Lee. Wind Design Optimization of a Solar-HALE Aircraft. *International Journal of Aeronautical and Space Science*, 2014.

[38] Mathias Aarre Maehlum. Energy informative, 2013.

[39] Werner Mansfeld. *Satellitenortung und Navigation: Grundlagen, Wirkungsweise und Anwendung globaler Satellitennavigationssysteme.* Springer, 2009.

[40] Pezhman Mardanpour and Dewey H. Hodges. Passive Morphing of Solar Powered Flying Wing Aircraft. Technical report, Daniel Guggenheim School of Aerospace, Georgia Institute of Technology, Atlanta, Georgia, 2012.

[41] S. Markgraf, M. Hörenz, T. Schmiel, W. Jehle, J. Lucas, and N. Henn. Alkaline fuel cells running at elevated temperature for regenerative fuel cell system applications on spacecrafts. *Journal of Powers*, 2012.

[42] LILTLULV MC MK, MTNL NO, and PLPTRORS SI. Metallhydridspeicher, reversibles brennstoffzellensystem sowie verwendung hierfür.

[43] Barnes Warnock McCormick, Barnes Warnock McCormick, and Barnes Warnock McCormick. *Aerodynamics, aeronautics, and flight mechanics*, volume 2. Wiley New York, 1995.

[44] Ernst Messerschmid and Ing Stefanos Fasoulas. Energieversorgungsanlagen. In *Raumfahrtsysteme*, pages 287–320. Springer, 2000.

[45] Stu Moment. Simple aerodynamics, part 6, 2004.

[46] Yoshio Nishi. Lithium-ion secondary batteries; past 10 years and future. *Journal of Powers*, 2001.

[47] John W. Norbury. Perspective on space radiation for space flights in 2020 - 2040. *Advances in Space Research, COSPAR*, 2010.

[48] World Meteoroligcal Organization. Cloud Classification, last update 2014.

[49] Pilotfriend. Fixed wing flight training, 2006.

[50] The Dreese Airfoil Primer. Reynolds number made easy, 2007.

[51] Volker Quaschning. *Regenerative Energiesysteme: Technologie - Berechnung - Simulation.* Carl Hanser Verlag GmbH Co. KG, 2013.

[52] Annabel Rapinett. A high altitude long endurance unmanned air vehicle. Technical report, Department of Physics, University of Surrey, Great Britain, 2009.

[53] András Sóbester and Alexander I. J. Forrester. *Aircraft Aerodynamic Design: Geometry and Optimization (Aerospace Series) [Kindle Edition].* Wiley, 2014.

[54] Ludwig Schiller, Jakob Ackeret, Albert Betz, O von Eberhard, Jakob Ackeret, and Jakob Ackeret. *Hydro-und aerodynamik.* Akademische Verlagsgesellschaft, 1932.

[55] Hermann Schlichting and Erich Truckenbrodt. Einführung in die aerodynamik des tragflügels. *Aerodynamik des Flugzeuges*, pages 353–390, 2001.

[56] Hermann Schlichting, Erich Truckenbrodt, Hermann Schlichting, Hermann Schlichting, Erich Truckenbrodt, and Erich Truckenbrodt. *Aerodynamik des Flugzeuges.* Springer Berlin, Heidelberg, 1969.

[57] Rod Simpson. *Airlife's World Aircraft: The Complete Reference to Civil, Military and Light Aircraft.* Grantham Book Orphans, 2001.

[58] F. Spurný. Radiation doses at high altitudes and during space flights. *Radiation Physics and Chemistry*, 2001.

[59] Obungsbuch Strdmungsiinecliaiiik. Technische strsmungslehre von l. boswirth strsmungsinecliaiiik a-z von h. herwig aerodynamik der stumpfeii ksrper.

[60] Strom Basiswissen- Informationszentrale der Energiewirtschaft e.V. Informationszentrale d. Elektrizitätwirtschaft (IDE) e.V., 2010.

[61] Flying techniques. Notions and basics, 2008.

[62] Dr. Axel Thielmann. Technologie-Roadmap Lithium-Ionen-Batterien. Technical report, Fraunhofer ISI, 2010.

[63] Airfoil Tools. E214, last update 2014.

[64] Lucien F. Trueb. *Batterien und Akkumulatoren: Mobile Energiequellen Für Heute Und Morgen*. Springer, 2013.

[65] Lucien F Trueb and Paul Rüetschi. Lithium-primärbatterien. In *Batterien und Akkumulatoren*, pages 52–61. Springer, 1998.

[66] Battery University. Supercapacitor, 2010.

[67] Wolfgang Weißbach and Michael Dahms. *Werkstoffkunde: Strukturen, Eigenschaften, Prüfung*. •, 2011.

[68] Wikipedia. Wolke, last update 2014.

[69] Gao Xian-Zhong, Hou Zhong-Xi, Guo Zheng, Liu Jian-Xia, and Chen Xiao-Qian. Energy management strategy for solar-powered hig-altitude long-endurance aircraft. *Energy Conversion and Management*, 2013.

[70] Gao Xian-Zhong, Hou Zhong-Xi, Guo Zheng, Fan Rong-Fei, and Chen Xiao-Qian. The equivalence of gravitational potential and rechargeable battery for high-altitude long-endurance solar-powered aircraft on energy storage. *Energy Conversion and Management*, 76:986–995, 2013.

[71] Li Li Zhang and XS Zhao. Carbon-based materials as supercapacitor electrodes. *Chemical Society Reviews*, 38(9):2520–2531, 2009.